University of Nevada

Reno

In-situ Leaching: The Effect of Temperature and Pressure on the Permeability of Uranium bearing Rock

A thesis submitted in partial fulfillment of the requirements for the degree of Master of Science in Mining Engineering

by

Everton Conrad Sequeira
"

December 1979

The thesis of Everton Conrad Sequeira is approved:

Thesis Advisor

Department Chairman

Dean, Graduate School

University of Nevada

Reno

December 1979

TABLE OF CONTENTS

ACKNOWLEDGEMENTS

The author wishes to express his sincere gratitude to the members of his committee, Dr. Y. S. Kim, Dr. Ross Smith and Dr. Philip Rymers, for their invaluable suggestions that made this thesis presentation possible.

To Dr. Y. S. Kim, Professor of Mining, Assistant to the Dean, and thesis advisor; whose suggestions, guidance and cooperation made this research project presentable.

To Professor Pierre Mousset-Jones, who took an active interest in the research project and provided assistance whenever needed.

To Mr. T. R. Nielsen, laboratory technician, dept. of Civil Engineering, who was instrumental in the laboratory set-up, and provided the necessary tools for the experimentation.

Last, but not the least, to the many friends and fellow students, who provided encouragement and assistance. Finally, the computer center, located in the Water Resource Building, for providing information on the Draft UCFMT, and Text Editor UCEDIT , that the author used, to flawlessly type out this thesis.

LIST OF FIGURES

ABSTRACT

This thesis concerns the insitu leaching of low grade uranium deposits that would be infeasible to mine by conventional mining methods. Initially, the report deals with the actual leach mining process, from well construction, to the extraction of values from the leach solution. The main area of research, however, centers around the permeability characteristics of the rock. The effect of temperature and pressure on rock permeability epitomizes this study, and is determined by laboratory testing. The purpose of this study is to observe the effect of these parameters on rock permeability and hence its leachability. The experimentation is carried out using Navajo sandstone samples to simulate the uranium measure rock. These samples are subjected to different temperatures of lixiviant (in this case, air), and injection pressures, and the coefficient of permeability is calculated from Darcy's law.

A mathematical model of the problem is presented in the literature review. This model incorporates the leaching process with the different variables associated with it including; oxidant concentration, velocities of flow of the lixiviant along the different streamlines, guard wells, dispersion of the lixiviant, and uranium concentration.

LIST OF SYMBOLS

A = area of cross section of the porous media, cm
C = concentration, gm/cc
d = average particle diameter, cm
D = molecular diffusion coefficient, sq cm/sec
E = Young's modulus of elasticity, kg/sq cm
F = formation resistivity factor,
G = shear modulus, kg/sq cm
h = height, cm
k = intrinsic permeability, micro m
Ka= coefficient of permeability, darcys
Kd= dispersion coefficient, cm/sec
L = length of the porous medium, cm
M = pyrite concentration, gm pyrite/gm rock
n = fluid viscosity, cP
P = pressure, atg
pd= drainage boundary pressure, kg/sq cm
pw= wellbore pressure, kg/sq cm
p = pore pressure, kg/sq cm
Q = volume flow rate ml/sec
r = radial distance from the well center, cm
rd= drainage boundary radius, cm
RI= 2% of the average distance between wells, cm
S = stress, kg/sq cm
Sc= confining pressure on core, kg/sq cm
Sf= stress due to horizontal loading, kg/sq cm
So= stress due to overburden, kg/sq cm
t = time, sec
U = dispersion, cm/sec
V = velocity, cm/sec
W = uranium concentration, gm uranium/gm rock
x,y = coordinate points, cm

Subscripts

1 = inlet
2 = outlet
m = mean
r = radial
θ = tangential
z = axial/vertical

Greek

α = a complex function of velocity appearing in the concentration balance,
β = a complex function of velocity appearing in the concentration balance,
γ = shear strain,
δ = stoichiometric coefficient, gm pyrite/gm oxygen
Δ = increment,
ε = uranium reaction rate constant,
ζ = oxygen reaction rate constant,
μ = fluid viscosity, gm/cm
ν = Poissons ratio of bulk sample,
ρ = density, gm/cc
σ = formation inhomogeneity factor,
τ = shear stress kg/sq cm
Φ = potential, atm
ϕ = porosity

INTRODUCTION

The purpose of this thesis is to investigate the effects of temperature and pressure on the permeability of uranium bearing rock.

The end result desired is a suitable directive that could be applied to leachable uranium deposits. This directive would determine how temperature and pressure of the lixiviant would affect the absolute permeability of the rock, and hence its leachability. The laboratory investigation is a simulation of the insitu leach mining process. The rock sample represents the uranium deposit present within the aquifer. The injection pressure is adequately represented by the inlet pressure generated by the compressor. The temperature conditions of the rock are simulated by an oven enclosing the sample.

The leaching kinetics are beyond the scope of the experimental study, but are presented nevertheless, in the theory of insitu leaching. Also presented with the insitu leaching theory is a mathematical model that describes the leaching process.

Statement Of The Problem And Scope Of Investigation

Insitu leaching techniques are being increasingly resorted to, owing to the current energy situation. Lower

grades of uranium deposits are being mined, and frequently they are infeasible to mine by conventional methods.

A considerable amount of practical experience has been gained in the industry by personnel who have been involved with insitu leach mining. Hence the author will not attempt to experiment with the actual leaching process.

Instead, work will be done to determine how the rock permeability is affected by lixiviant temperature, and injection pressure.

Some temperature studies on rock permeability have been done in the petroleum industry, but none of it is relevant to the leach mining of mineral values, the author attempts to tie in the petroleum experience with leach mining.
No injection pressure studies on rock permeability have been done to the authors knowledge.

The laboratory tests do not involve the chemistry of leaching; only the physical aspects of leaching are investigated.

Importance Of The Problem

In insitu leaching, the ease with which the fluid flows

through the rock is one of the factors that are involved in the profitability of the undertaking.

A study on the effect of injection pressure and lixiviant temperature on rock permeability, may indicate a need for modifying the physical properties of the lixiviant before it is dispatched into the rock through the injection well.

Temperature studies on rock permeability that have been done in the past, were mostly applicable to petroleum and related products, these studies are reviewed in the literature survey and where possible, results are correlated to insitu leaching. Injection pressure studies on permeability have not been uncovered by the author. For this reason an extensive laboratory program was set up and a model developed to study these parameters.

The model may seem ineffective as compared to site conditions. No attempt is made therefore, to present hard and fast rules that can be applied to the field. It may be pointed out, however, that if the laboratory tests indicate a relationship between the permeability of the rock and the lixiviant temperature and pressure; on site rock testing to determine the most favorable temperature and pressure that the lixiviant may be subjected to, can be justified.

Factors present insitu such as faults, folds, joints and other discontinuities cannot be duplicated in the laboratory, hence the model is not claimed to be adequate.

INSITU LEACHING

The Leaching Process

The insitu leaching process consists of the injection of a lixiviant (suitable leach solution) into the ore zone contained within the aquifer, oxidizing, complexing and mobilizing the uranium; followed by the recovery of the pregnant solution by pumping to the surface through the recovery or production wells. Some common well configurations are shown in figure 1. Dilute concentrations of ammonium carbonate bicarbonate, or sulfuric acid, can be suitable lixiviants.

Once the uranium minerals have been complexed and mobilized, they follow the flow gradient in the ore zone at a strategic location, at which a production well has been sunk. Submersible pumps transfer the pregnant solution to the surface for processing. The residual (uranium barren) solution from the ion exchange process is recirculated to the well field. The ion exchange is a cyclical process, and is done in two steps; the loading or the absorption step, and the elution step. During the loading step the pregnant leach solution contacts the ion exchange resin and the uranium is selectively absorbed. When a suitable uranium loading has been achieved the resin is cycled to the elution

step. During elution a chemical solution strips the resin of its uranium, the resulting product solution is termed the eluate, and the eluted solution is cycled back to the loading operation.

Concentration and purification take place during the ion exchange operation. Ion exchange equipment arrangements that have been used in insitu leaching operations are of several types. These include fixed-bed columns which use batch-type operational procedures, and multiple compartment column systems that operate with semi-continuous counter current flow of both the solutions and the resin.

The eluate is relieved of its uranium by precipitation, and the recovery procedure is dependent on the type of solution used for the elution step. For example, if the uranium is eluted with an acidic salt solution, the precipitation can be made with direct neutralization with ammonia. The precipitate is yellow in color, and comprises mainly of ammonium diuranate, generally called yellow cake. If however, an alkaline carbonate eluting solution is used, the yellow cake cannot be directly obtained by ammonia precipitation. The ammonium carbonate complex must be destroyed before yellow cake precipitation or incomplete precipitation will result. An acid such as HCl would destroy the carbonate complex, and permit uranium

precipitation by ammonia neutralization. Thickeners and filters next separate the yellow cake from the residual solution. The yellow cake is then dried, and packaged for shipment.

Well Construction Methods

A production well must perform as expected, or a second well will have to be drilled. This would double costs.

Geology and hydrology of the formation, experience and sometimes budgeting constraints have been used in the past to design wells. The end purpose, no matter what the system used, is the same. The wells should be so constructed as to isolate aquifers above and below the ore zone. Intermingling of natural ground water from more than one zone should be prevented. During the actual leaching operations the leach solution should be confined to the aquifer within the ore zone, and should not travel up, around, or below the casing to the other aquifers. This is for both environmental and economic reasons.

Commonly, wells are drilled to a depth just below the ore zone, or to the base of the ore-producing sandstone. Rotary drilling is most commonly used. Although, drilling fluids, foam and air drilling and reverse circulation

techniques have been experimented with by some operators.

Field experimentation cannot be over emphasised, because the success of most of these methods have depended on the geologic conditions at a particular deposit.

Drilling techniques must be investigated; various drilling fluids have been experimented with. Water, guar gum and bentonite base polymers have been tried with varying degrees of success.

After drilling, the hole must be cleaned with mechanical brushes, sidewall scrapers, or chemicals, to rid the wall of the sidewall cake formed during drilling. The actual method used would depend on the geologic conditions present.

The next step is to lower PVC (Poly Vinyl Chloride) pipes into the well. Usually a PVC screen, or slotted casing of the same diameter is attached to the bottom. The PVC pipes are lowered into the hole until the PVC screen is opposite the ore zone. A subjoint consisting of a plaster of paris plug and a wooden cap is usually attached above the screen. The purpose of the cap is to exclude foreign material, especially cement, from accumulating on the screen during the cementing operation. In order to cement the

annular space between the casing and the drill hole, weep holes are drilled above the plug and through the casing. The screen is protected from downward moving cement, by a cement or shale basket just below the weep holes. In addition, one or more centralizers are placed at 20-foot intervals up the casing to ensure a uniform cement flow and thickness around the casing. Finally, cement (usually type II construction or Class A or B Portland cement) is pumped through the casing, displacing the water and drilling mud in the annulus until the cement is circulated to the surface. Additives such as bentonite, mica, cellophane flakes or fiberglass have been tried to ensure a better cementing bond. Excepting for the last 10 to 30 feet above the plug, water is usually pumped down the hole to displace the cementing slurry. Usually from 10 to 100 percent additional cement is required to complete the cementing operation, depending on the site conditions. Before the cement reaches maximum strength, usually from 5 to 10 hours, the cement column and the wooden plug are drilled out.

The result of this method is that the casing is cemented through all of the overlying formations and aquifers, thus preventing vertical communication between the ore zone and the other aquifers. A suitable well developmental procedure must be used on completion of the well, such as flushing, jetting, air-lifting or surging,

including gravel packing and the use of chemicals. Figure 2 shows the section of a well constructed in the manner described. Other well construction methods are described in {1}.

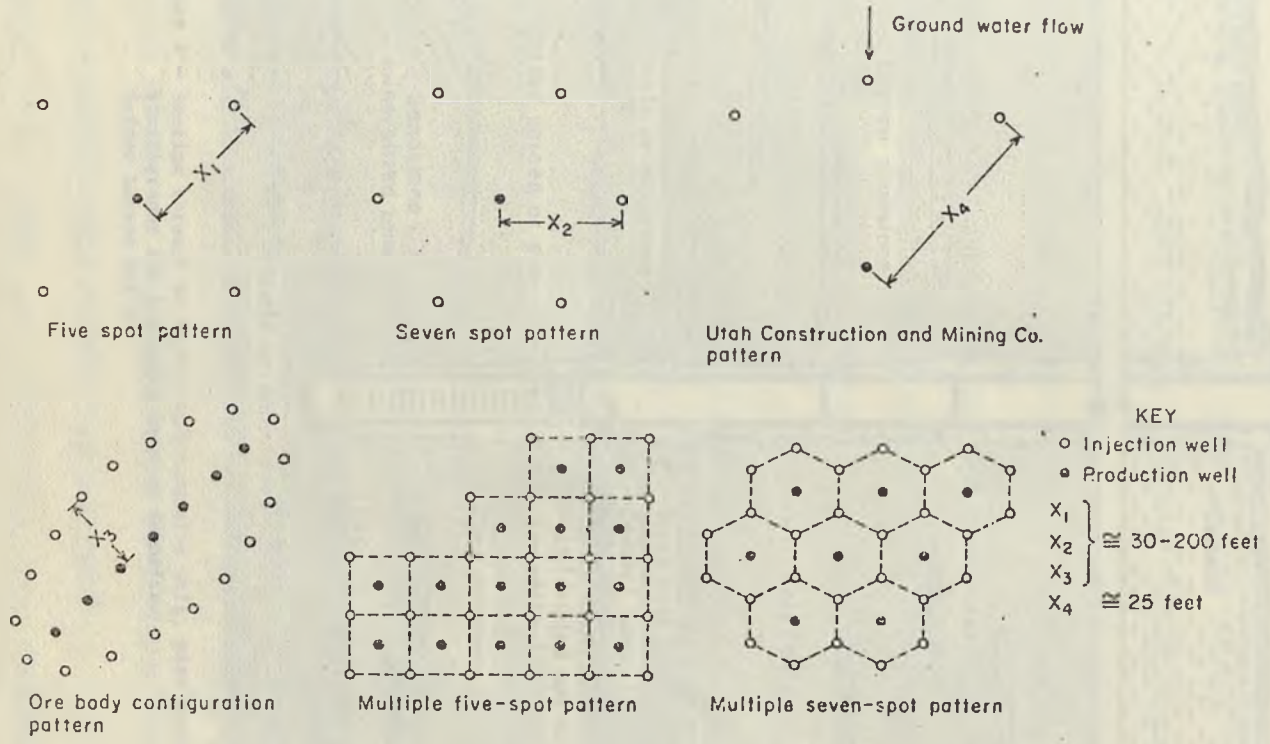

Figure 1 - Well configuration patterns.
(after Larson, ref 1)

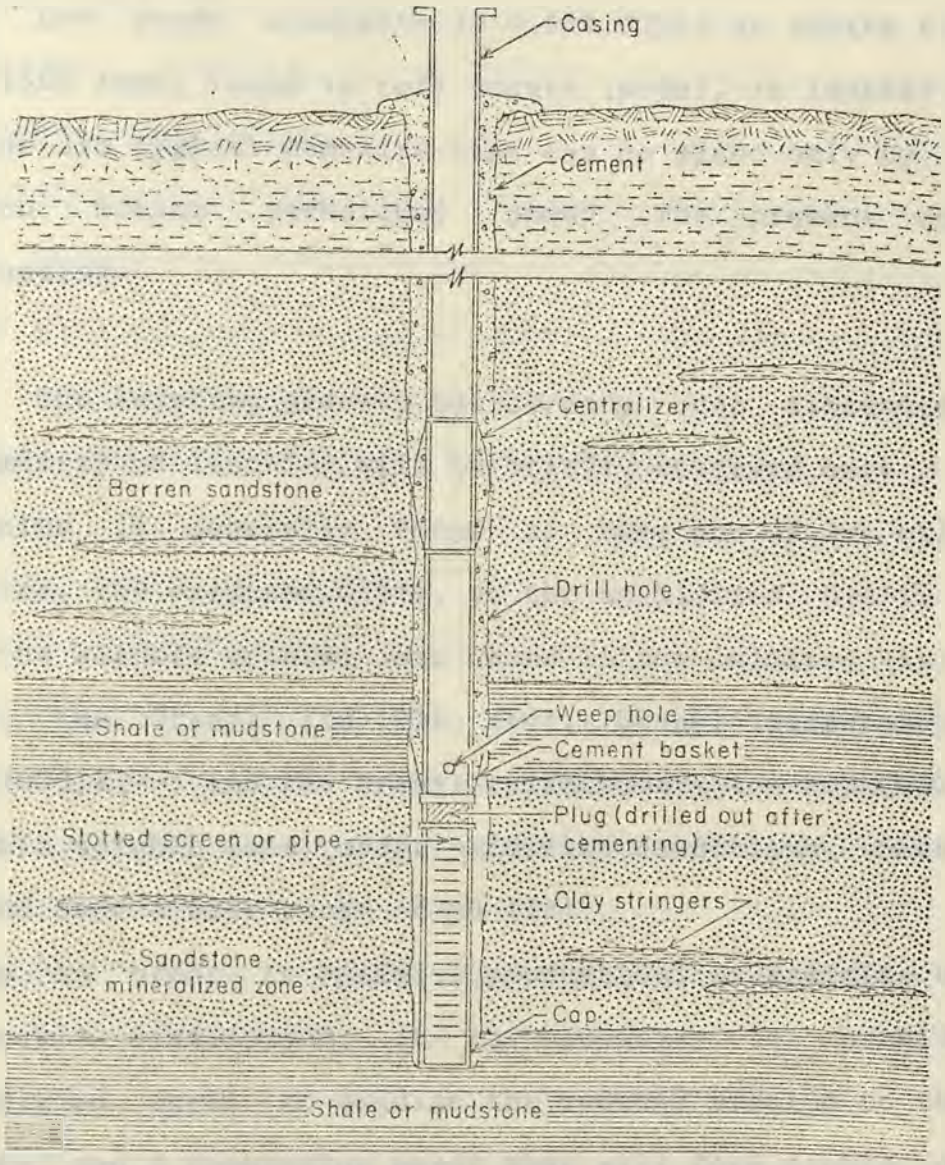

Figure 2 - Section through an injection/production well, with typical stratigraphy for low grade uranium deposits. (after Larson ref 1)

Mathematical Modeling

Low grade uraninite (< 0.05% U3O8) at depths from 100 to 1500 feet, found in roll fronts (pods), in loosely packed sands are typical deposits that can be mined only by insitu leach mining techniques under the present economic situation.

The leaching process has already been discussed, the chemistry of leaching will be briefly reviewed here.
Uranium is generally found to have one of two oxidation states, the oxidized U(6+), or the unoxidized U(4+). Some of the soluble uranium ions found in the oxidized (6+) state are; the Uranyl ion UO2 (++), Uranyl dicarbonate ion, UO2(CO3)2(--) and the Uranyl tricarbonate ion UO2(CO3)3(4-). Stable soluble ions, under oxidizing conditions, have been found over a wide range of pH {15}.
Thus in order to optimize production, or maximize uranium minerals dissolution, it is necessary to provide an oxidizing agent to oxidize the reduced uranium to the (6+) state, and a complexing agent that will form stable complex ions with U (6+). The following reactions are exemplary:

$$UO_2 + H_2O_2 = UO_3 + H_2O \quad \text{(oxidation)}$$

$$2H^{(+)} + UO_3 + 3CO_3^{(2-)} = UO_2(CO_3)^{(4-)} + H_2O \quad \text{(dissolution)}$$

Hydrogen peroxide is the oxidant, which could be replaced by

air, sodium chlorate, or pure oxygen. The objective of the insitu leaching project is to recover a large part of the mineral value in a reasonable length of time. This entails efficient placement of production and injection wells and sometimes guard wells.

This mathematical model deals with the above situations and also production rates, effect of oxidant concentration and other questions concerning the insitu leaching process.

Assumptions To Validate The Flow Model

The flow is assumed to be single phase and two dimensional, this facilitates the application of the well known Laplace line source and sink equations for an incompressible fluid flowing through a porous medium as a function of location and volume rates of production and injection wells.

$$\Phi(X,Y) = \Phi_m - u/(4\pi kh)\,\Sigma Qi\,\ln\{(X-Xi)^2 + (Y-Yi)^2\} \text{ --- (5)}$$

Differentiating expression (5) with respect to X and Y to obtain vectorial components in those directions yield:

$$Vx(X,Y) = \{-1/(2\pi h)\}\,\Sigma Qi(X-Xi)/\{(X-Xi)^2 + (Y-Yi)^2\} \text{ --- (6)}$$

$$Vy(X,Y) = \{-1/(2\pi h)\}\,\Sigma Qi(Y-Yi)/\{(X-Xi)^2 + (Y-Yi)^2\} \text{ --- (7)}$$

Let us now assume an average distance between wells, and RI to be two percent of that distance, next find the

resultant velocity as,

$$V(X,Y) = (Vx^2 + Vy^2)^{\frac{1}{2}} \quad \text{--- (8)}$$

The time taken by a fluid particle to traverse the distance RI is:

$$\Delta t = (RI)/V(X,Y) \quad \text{--- (9)}$$

The new coordinates of the particle along the streamline are:

$$Xi+1 = Xi + Vx(X,Y)\ \Delta\ t \quad \text{--- (10)}$$

$$Yi+1 = Yi + Vy\ (X,Y)\ \Delta t \quad \text{--- (11)}$$

This process when repeated for each streamline of each production well, gives a trace of the streamlines between production and injection wells.

Once the streamlines have been defined, the pressure drop along them can be calculated. The next assumption is in assigning equal pressure increments, and labelling them as nodes, to be used in developing a finite difference analog of the concentration balance. The fluid velocity is recorded at each node to be used later in finite difference equations.

In order to calculate the actual velocity of flow along a streamline, the thickness of the formation must be known at each point along the streamline. These values of thickness are entered over the area of the pod using a grid system (figure 3). Thus the fluid velocity is adjusted at

each node and used in the calculations for both uranium and oxidant concentrations.

Since the area of the uranium pods is small compared to the area of the host rock, the lixiviant must be prevented from escaping from the uranium pod zone. In other words, the lixiviant must be bounded. This is achieved by suitably locating guard wells to create a no flow boundary around the area of the pods. Proper injection rates from guard wells achieves this end. An infinite combination of guard wells exist to produce adequate bounding, and economics is the deciding factor. The streamlines, before and after the introduction of guard wells, is shown in figures(4) and (5).

After the calculation of velocities have been completed and stored at each node, the concentration of uranium at each node must be defined as a function of time. This can be done by using a concentration balance equation in the axial, as opposed to the radial, direction.

$$-Ux\,\partial c/\partial x - Uy\,\partial c/\partial y + (\partial/\partial x)(Kxx(\partial c/\partial x) + \partial/\partial x(Kxy(\partial c/\partial y)) + (\partial/\partial y)(Kyx\partial c/\partial x) + \partial/\partial y(Kyy\partial c/\partial y) - R = \Phi\,\partial c/\partial t \quad \text{---- (12).}$$

Neglecting the dispersion perpendicular to the flow equation-(12) can be converted from rectangular coordinates to potential and streamfunction coordinates, thus:

$$\{(\mu/K)\{U^2 - 2(UxUy)/U^2\ Kl(\partial/\partial y)(Ux) - Kl(Ux^2/U^2)(\partial/\partial x(Ux) + (Uy^2/U^2)\,\partial/\partial y(Uy))\}\}\,\partial c/\partial\phi +$$

$(U^2\ \mu^2/K^2)\ Kl\ \partial / \partial\phi(\partial c/\partial\phi) - R = \Phi\partial c/\partial t$ ---- (13)

Define

$\alpha = (\mu/K)\ \{U^2 - (2UxUy/U^2\ Kl\ \partial/\partial y\ (Ux) - Kl\ ((Ux^2/U^2)\ \partial/\partial x(Ux) + Uy^2/U^2\ \partial/\partial y(Uy))\}$ ---- (14)

$\beta = U^2\ (\mu/K)^2\ Kl$ ---- (15),

$Kl = D/F\phi + 0.5V\sigma P$ ---- (16).

This is the expression for longitudinal dispersion and was described by Perkins et al {14}

All the terms in (15) and (16) are known from the streamline generator or can be calculated. So, the concentration balance, equation (13) can be reduced to

$\alpha(\partial c/\partial\phi) + \beta(\partial^2 c/\partial\phi^2) - R = \phi(\partial c/\partial t)$ ---- (17).

The R term is the rate expression for either uranium or mineral oxidation. Φ is the potential function, which for a horizontal system is measured along the streamline. The form of the reaction rate used by Bommer and Schechter {15} was $Rur = \varepsilon(Wur - Wrur)(1-\phi)\rho$ ---- (18).

ε depends on a number of factors including oxidant concentration, but Bommer and Schechter used an experimentally determined relationship between the rate constant (ε) and the peroxide concentration.

Equation (17) is solved for each streamline at selected times. It is solved using a fully discrete finite difference approximation, with an unconditionally stable Gaussian row reduction technique. The output from the

balance is the uranium concentration at each node of each streamline at every time step, in gm/cc. The solution of equation (17) yields the uranium concentration at each well bore.

Modeling Considerations

Delayed uranium production is caused by other minerals present in aquifers, such as pyrites. These minerals compete with uranium for the oxidant. The rate expression that takes into account this consideration is

$Ro = \zeta MCo/\delta$

The oxidant consuming mineral concentrations are initially stored and used in the rate expression.

As the reaction proceeds,

$$dM/dT = -\delta Ro \quad \text{--- (20)}$$

This equation when integrated yields (19) and the mineral concentration is allowed to decrease with time. Thus, given the oxidant concentrations left at each node, after reactions with oxidant consuming minerals, the appropriate constant ε , can be located and used in equation-(16).

The model also accounts for the fact that most reservoirs are not chemically homogeneous systems. This

nonhomogeneity is accounted for by storing the differences in reservoir thickness in the grid system, the velocity approximation can be used to provide concentration variances.

Gross changes in permeability can be accounted for by adjusting the thickness to maintain a correct Kh value. The portions of the streamline that lie outside the uranium bearing area do not contribute any new uranium to the system. This zone may, however, contain pyrite and thus continue to consume oxidant. To account for these setbacks, the following procedure is followed. The cross product of the two vectors is determined. The first vector passes through the node and the nearest boundary point to that node. The uranium bearing area is described by a finite set of discrete boundary points. The second vector passes through the closest boundary point and the next point along the streamline taken in a clockwise direction, as shown in figure (6). If the cross product is positive, the node is inside the pod and if negative, the node is outside the pod and no uranium production is calculated.

The inadequacies of this method are displayed when the node, the nearest boundary point and the next point are all on a line, forming an angle of 180 degrees. When this occurs, the cross product is zero and no decision can be

made. In this event, the model uses the boundary point behind the closest boundary point to form the first vector and that point and the closest boundary point to form the second vector.

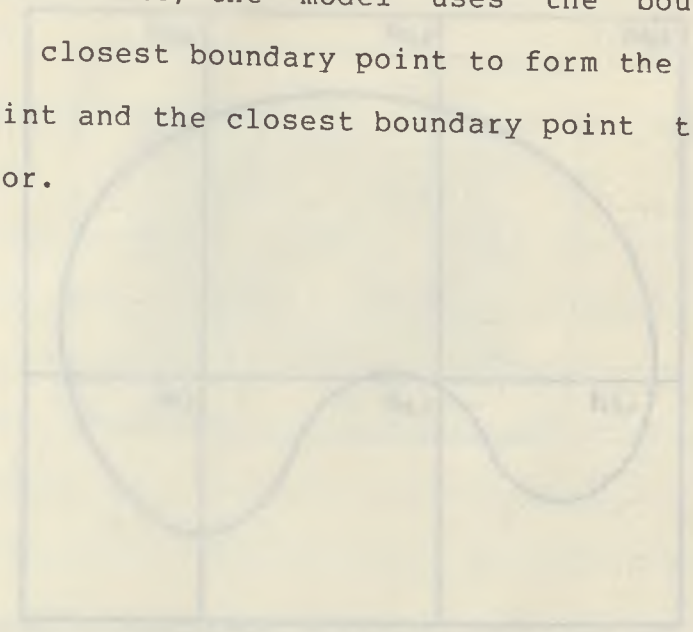

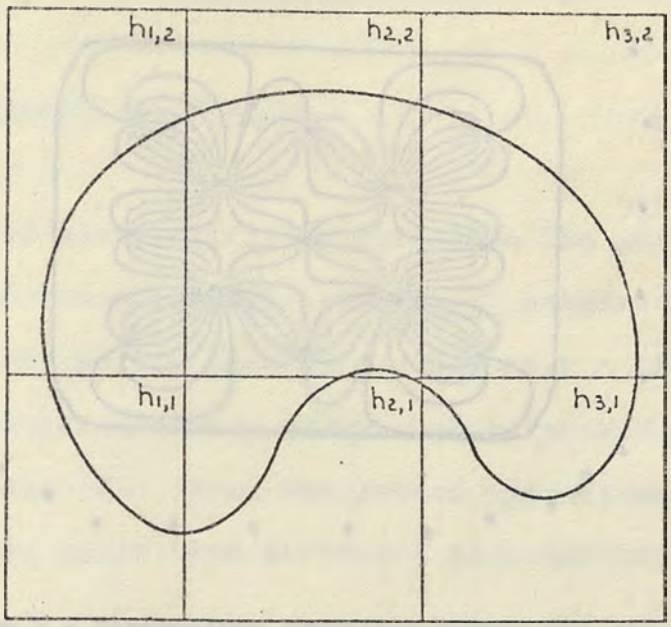

Figure 3 - Grid system over the area of the pod.
(after Bommer and Schechter ref 17)

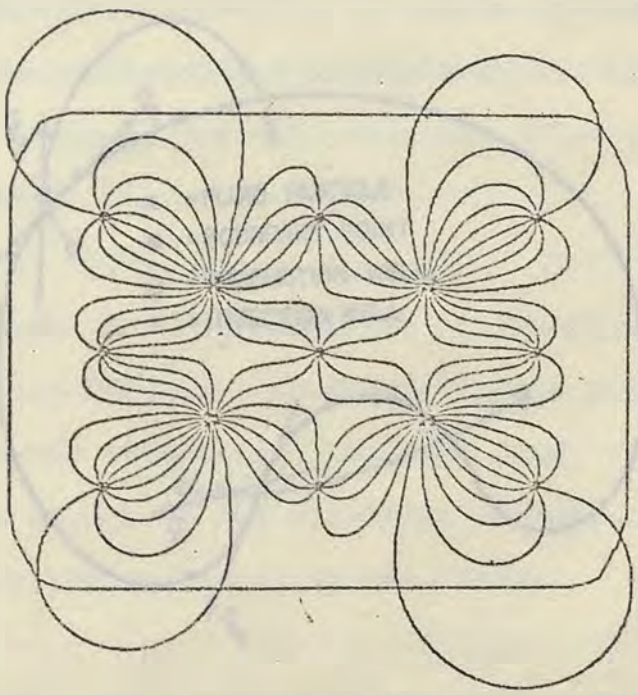

Figure 4 - Streamline before the introduction of guard wells (after Bommer and Schechter, ref 17)

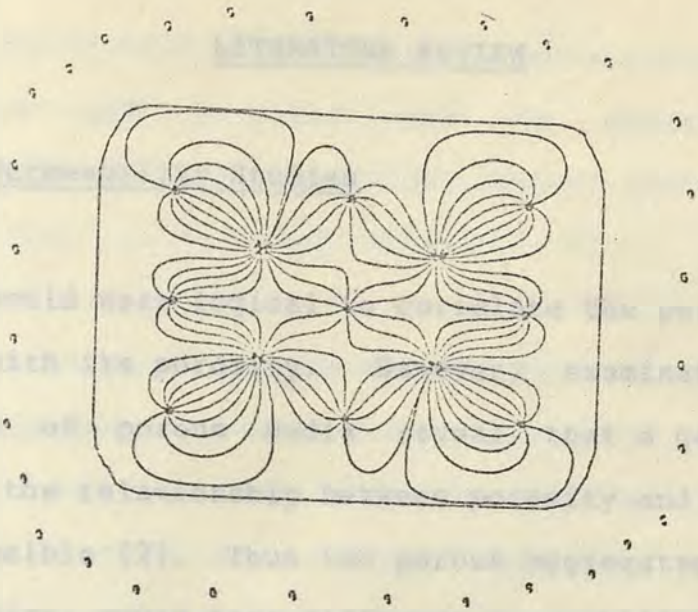

Figure 5 - Streamlines contained within the pod after introducing guard wells. (after Bommer and Schechter, ref 17)

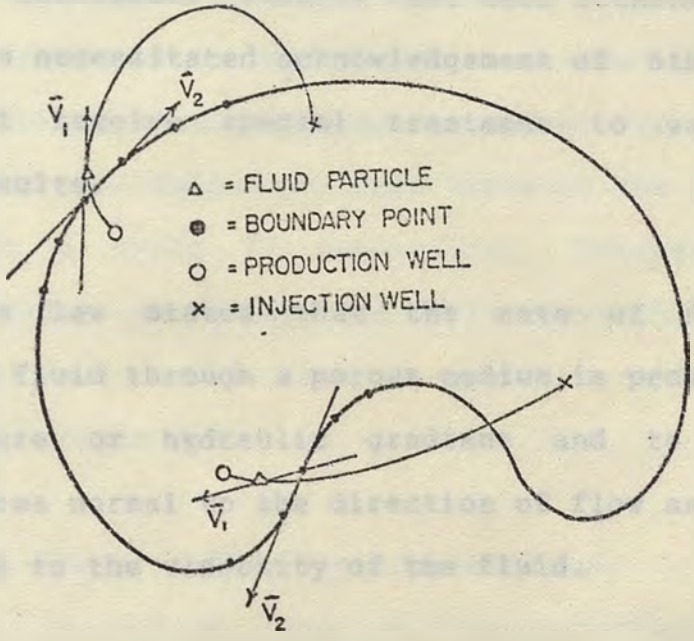

Figure 6 - Vector analysis to determine location of the fluid particle, relative to the pod boundary. (after Bommer and Schechter, ref 17)

LITERATURE REVIEW

Previous Permeability Studies

It would seem logical to correlate the permeability of a sample with its porosity. However, examination of the structures of porous media reveal that a generalization regarding the relationship between porosity and permeability is not feasible {2}. Thus two porous aggregates having the same porosity, could have different permeabilities.

Studies {3} have been done to attempt to find a relationship between permeability and porosity. Where apparently successful results have been attained most such efforts have necessitated acknowledgement of other factors which must receive special treatment to validate the obtained results.

Darcy's law states that the rate of flow of a homogeneous fluid through a porous medium is proportional to the pressure or hydraulic gradient and to the cross sectional area normal to the direction of flow and inversely proportional to the viscosity of the fluid.

The encompassing limitations in the foregoing definition involve generalizations and idealisms. It is the

the purpose of this thesis to investigate the parameters of temperature and pressure and to determine their relationships with permeability, other factors remaining constant.

A limitation in Darcy's law, is the reference to the term homogeneous fluids, this means that heterogeneous fluids may not be used with the express intention of satisfying Darcy's law. Darcy used water as a fluid and unconsolidated sand as the porous medium to derive his formula.

The use of the term fluid, in Darcy's law, implicitly means any fluid that does not interact with the porous medium. Insitu leaching fluids, as has been already discussed, do react with the porous medium, but, the ratio of the reactive medium surface areas to the body of rock involved as a whole is negligible. Furthermore, such reactions would generally tend to increase the porosity of the medium, and would have a positive effect on the leachability of the ore.

Darcy's law is ordinarily expressed as:

$$Ka = (Q\ n\ L)/A(P1-P2) \quad \text{--- (1)}$$

where;

Ka = coefficient of permeability in Darcy's,

Q = volume flow rate in ml/sec,

n = fluid viscosity in centipoises,

L = length of the porous medium in cm,

A = area of cross section of the porous medium,

Pl = pressure at the outlet, and

P2 = the inlet pressure.

However, if the fluid happens to be a gas, certain adjustments must be made in calculating permeabilities. These adjustments take into account gas slippage, and consider the pressure at which the volume rate of fluid flow is measured.

Mean pressure must be used in the calculations instead of the inlet or outlet pressures, because it is this pressure that causes the gas to flow across the sample.

Now if Pl is the upstream pressure and P2 is the downstream pressure;

$$Q2\ P2 = Qm\ Pm \quad \text{--- (2)}$$

where,

$$Pm = (P1+P2)/2,$$

Qm is the volume rate of flow corresponding to the average pressure,

and Q2 is the volume rate of flow corresponding to pressure

P2.

Thus, Qm would have to be substituted in equation (1) for Q and the equation would become:-

$$Ka = (Qm\ n\ L)/A\ (P2-P1) \quad --- \quad (3)$$

If a comparison is to be made between permeabilities using a gas as the measuring fluid, or a liquid, another consideration must be made. This is the molecular slippage of the gas past the walls of the channel, and attributable to Klinkenberg's equation {4} or,

$$Ka = Ko(1+b/Pm) \quad --- \quad (4)$$

where,

Ka = the permeability coefficient at some particular mean pressure,

Ko = permeability coefficient at infinite mean pressure,

b = constant = M/Ko,

M = slope of the line obtained by plotting Ka versus 1/Pm,

and,

Pm = (P1+P2)/2 = mean pressure across the sample.

Ko at infinite mean pressure is found to be the same as the permeability of the medium using liquids as the measuring fluid, allowing for experimental error. Thus graphical extrapolation of the plot of Ka versus 1/Pm would

yield Ko on the intercept of the Ka axis at infinite mean pressure or, at 1/Pm.

Another limitation of Darcy's equation is that it is invalid outside of the viscous flow range, the expression of Klinkenberg, however, allows for this drawback and permits the application of Darcy's law outside of the viscous flow range.

The permeability coefficient is constant in the viscous flow range and there exists a linear relationship between Ka and 1/Pm outside the viscous flow range.

Dolch {5} used air as the fluid and a decay phenomenon approach as a means of measurement; he conducted permeability studies on four Indiana limestones. Water has been used in the past to conduct permeability studies, but since it reacts with many of the minerals present, it could significantly affect the permeability value of the measured medium.

Weinbrandt and others {6} found that the absolute permeability decreased with temperature increase, this test was performed using water as the fluid and 100% water saturation of the samples. The average permeability decreased with a temperature increase from room temperature

at 80 degrees F to 175 degrees F.

This test had the sample confined by a pressure of 2000 psi. It was observed that the permeability decreased smoothly with an increase in temperature but the decrease becoming less prominent at the higher temperature.

Muscat {7} discusses a permeability measuring device, that employs dry air as the fluid medium.

Larson et al {8} devised and utilized equipment that employed dry air as the measuring medium.

Zoback and Byerlee {9} studied the effect of effective stress on permeability. They found that the permeability of Berea sandstone decreased with the increase in confining pressure and increased with the increase in pore pressure. They noted, however, that the pore pressure had a significantly larger effect than the confining pressure on the permeability of the sample. The key to their study was an understanding of the flow properties of reservoirs under stress.

Several investigators, {10}, {11} and {12} have suggested that permeability is dependent only on the effective stress (S - p); that is permeability is dependent

only on the difference between the hydrostatic confining pressure (S) and the pore pressure (p).

This investigation would throw light on the permeability of rock as affected by the pressure exerted on the leaching fluid (influent).

Past research was connected with the extraction of petroleum from permeable rock.

Insitu leaching involves injection of a suitable lixiviant into the rock, followed by the extraction process as in petroleum.

The results obtained by Zoback and Byerlee further indicated that permeability is not a simple function of effective stress, rather pore pressure has a considerably greater effect on permeability than does confining pressure. Also, for a constant confining pressure (solid lines in figure 7), permeability increases dramatically with increasing pore pressure. These results were for fluid flow normal to the bedding planes of the rock. Permeability measured parallel with the bedding planes (figure 8) indicated a similar result, with the permeabilities being naturally higher. Comparison of figures (7) and (8) indicate the anisotropic nature of the sandstone. When flow

is parallel to the bedding planes two effects are noted; firstly, that permeability is considerably higher, and secondly, the effects of pore pressure and confining pressure are more nearly the same. The results obtained from Zoback and Byerlee's studies indicated the following expression:

$K(p,S) = Ko + a(bp-S)$,

so that Ko, the intrinsic permeability, is found when $(bp-S) = 0$. They found that in each of the cases there existed constant values for a and b, when permeability was measured in the direction normal to and parallel to the bedding planes. In Berea sandstone, for flow normal to the bedding planes, the pore pressure was found to have four times the effect of confining pressure.

In related work, Vairogs et al {12} studied the effect of rock stress on gas production from low permeability reservoirs. They indicated that the lowering of pore pressure as gas is produced causes an increase in the confining stresses on the reservoir rock, causing compaction, and hence, a reduction of the effective pore diameters, resulting in a decrease of the permeability. Studies conducted by McLatchie et al {13}, for a core of less than 0.1 mD permeability, showed that stress had a relatively greater effect on this rock sample of low permeability, than on other cores of high permeabilities. A

possible explanation of this phenomena is that very tight cores have smaller pore diameters. Increase in the applied compressive stress would cause the pores of smaller diameter to decrease their flow capacity proportionately more than that of larger pores. Vairogs et al {12}, drew the following conclusions:

(1) Very tight rocks are affected by stress more than rocks having a higher permeability value.

(2) The permeability of a rock depends complexly on confining pressure. Fractures, shale streaks and other rock heterogeneities, accentuate the permeability reduction due to stress.

They incorporated the stress effect on permeability into a mathematical model, for gas flow, based on a theoretical analysis of the stress state around a well bore.

The mathematical implications of theirs, and others, can be found in the Appendix.

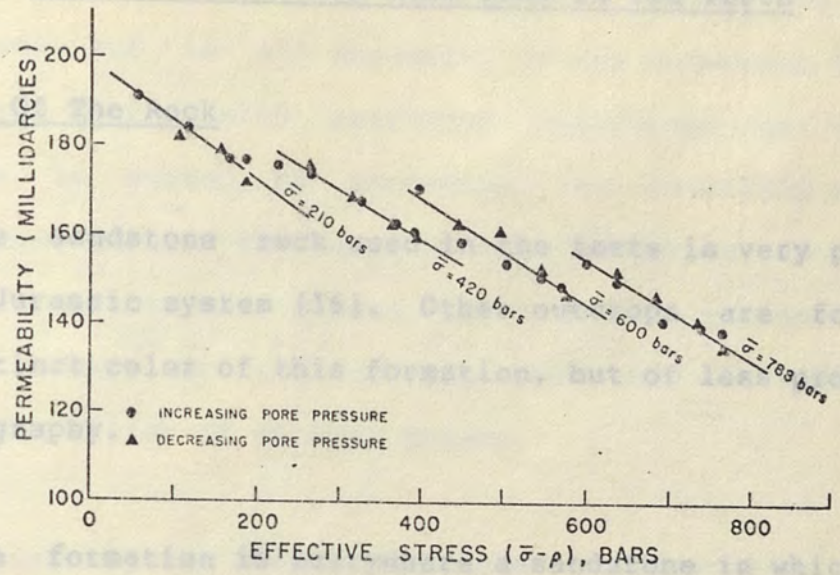

Figure 7 - Permeability and effective stress; measured parallel to the bedding planes.
(after Zoback and Byerlee, ref 9)

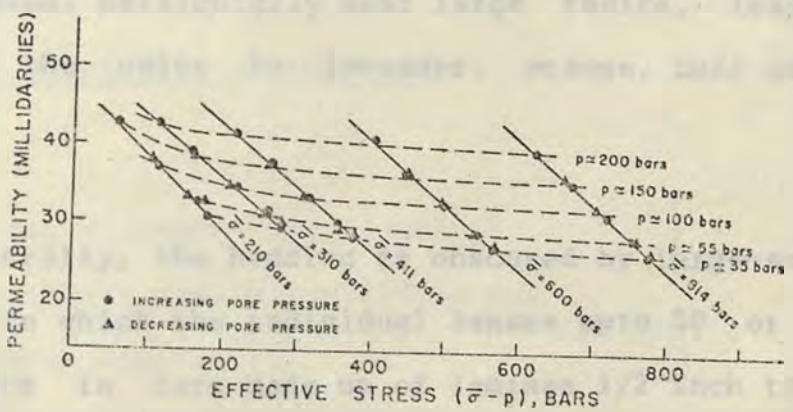

Figure 8 - Permeability and effective stress; measured normal to the bedding planes.
(after Zoback and Byerlee, ref 9)

DESCRIPTION OF THE ROCK USED IN THE TESTS

Geology Of The Rock

The sandstone rock used in the tests is very probably of the Jurassic system {16}. Other outcrops are found of the distinct color of this formation, but of less prominence in topography.

The formation is everywhere a sandstone in which fine- to medium-sized grains, mainly of quartz, are well rounded and in large part frosted. Iron oxide and minor calcium carbonate cement the grains weakly; most of the rock is friable. Most of the sandstones (including that used in the experimentations) are uniformly brick red in color; but in many places, particularly near large faults, leaching has changed the color to lavender, orange, buff and whitish gray.

Generally, the bedding is obscured by large-scale cross bedding in which the individual lenses upto 20 or 25 feet thick are in turn made up of laminae 1/2 inch to 2 inches thick. Ripple marks occur locally, but are not common. The rock weathers into grotesque forms which give the formations a distinctive appearance.

The Aztec sandstone is conformable along the Chinle formation; but in all exposures of the sandstone in Clark county the contact with overlying cretacious or tertiary deposits is marked by unconformities, generally angular. The maximum exposed thickness of the sandstone is 2000 - 2500 feet, but in many places, the formation is considerably thinner. Part or all of the formation has been eroded before deposition of younger strata.

Apparently the Aztec sandstone represents a western extension of the Colorado Plateau. Although no distinctive fossils have been found in the sandstone, either in the Plateau or in Southern Nevada, the formation is dated tentatively as Jurassic on the basis of its stratigraphic position.

Physical Properties of the Rock

St (tensile strength)=504.53 psi

Sc (compressive strength)=7123.10 psi

(poissons ratio)=0.25

E (Young's modulus)=2,000,000 psi

App. Porosity=11%

Thermal Properties

D (diffusivity)=0.0578 ft /hr=Tk/(c)

f (thermal expansion, linear)=0.0000008 % 1/degree C,

Kt (thermal conductivity)=8.2 cal/cm/sec/deg C.

EXPERIMENTATION

Experimental Design

The experimentation required apparatus that had temperature and pressure variation possibilities. A compressor with a pressure range from 0 to 500 psig was readily available. The temperature variable had to be introduced into the setup.

To obviate major experimental redesigning, it was decided to introduce an oven into the set-up. A long copper tube was used to connect the sample holder (containing the sample) and the pressure guages, the tube passed through a hole drilled in the roof of the oven, and was connected with the sample holder. The oven had a temperature range from 0 to 300 degrees C. In order to ensure that the sample was kept under isothermal conditions throughout the testing, the inlet to the sample was extended into the oven before connecting with the sample holder.

The inlet/outlet copper tubes were joined to the sample holder with air tight connectors. The oven temperature was monitored by a thermometer that was inserted through the same holes that the copper tubes passed through. The copper tube was next connected by plastic tubing to the gas

volumeter (wet test meter) which read the volume of air flowing through the sample. The gaps around the drill hole were sealed with asbestos. The experimental setup is shown in figure (18). The air tightness of the setup was determined by using an impervious blank disk.

Procedure

Sample Preparation

Step I

Core samples were drilled from the previously described rock, using a diamond drill press (figure 9). In order to avoid damaging the samples, care was taken to use minimal and uniform pressure on the drill handle. The cores obtained from the sandstone rock were 2.5 cm. in diameter, and about 12 cm in length, figure 10 depicts one of the cores obtained from the sandstone rock, using the diamond drill press.

Step II

The cores were then washed, dried and inserted into a

polyethylene sleeve. The core and the polyethylene sleeve were held together by Elmer's epoxy resin and epoxy hardener cementing bond (figure 11). The sheathed sample was then left undisturbed for at least 24 hours, to reach its maximum strength.

Step III

The next step in the process was to saw disks off the sheathed core. This was achieved by a rotary blade saw (figure 12). The disks were about 1.5 cm in thickness, and 2.5 cm in diameter, see figure 13. The samples were now ready for the next phase of laboratory work, i.e. testing.

Sample Testing

Test I

The first test was performed at room temperature, which was 24 degrees C. The compressor was turned on until the accumulator reached peak pressure, and the motor was automatically shut off. This procedure reduced pressure fluctuations in the model.
Next, the pressure valve was opened gradually until the guage showed a reading of 25 psi (1.7007 atg). This meant

that fluid (air) was flowing through the rock at an injection pressure of 25 psi, at 25 degrees C.
The fluid passing through the rock was measured by a wet test meter.
The pointer of the wet test meter was set to zero, and the flow quantity was timed by a stop watch, this was done to determine the flow rate of the lixiviant through the rock. Ten minutes was found to be sufficient, to accurately measure the flow quantity. During the entire time of flow, the pressure guage was constantly monitored, to note any fluctuations.
Thus, the volume of flow was recorded, and the value of permeability calculated for an injection pressure of 25 psig and an air temperature of 24 degrees C, using expression - (3).

The injection pressure was stepped up to 35 psig and the entire process was repeated as above.

Thus, permeability of the rock was calculated for injection pressures of 25, 35, 45, 55, 65, 75, 85 and 95 psig; at an air temperature of 24 degrees C (room temperature).
For each pressure level, a different rock sample was used.
The results obtsined from test I are shown in table I

Test II

The second series of permeability calculations were done for an air temperature of 41 degrees C.

The procedure followed was the same as outlined in test I, the results are depicted in table II.

Tests III, IV, and V were performed for air temperatures of 57, 69 and 86 degrees C, and the results therefrom are shown in tables III, IV, and V, respectively.

The oven containing the sample was maintained at constant temperature for at least 8 hours, to maintain proximate isothermal conditions.

The readings taken for each test were those of pressure, temperature, volume of air flowing through the sample, the time of flow, and the ambient atmospheric pressure.

In order to ensure accurate wet test meter readings, the initial tests at room temperature were performed over prolonged periods of time. These tests indicated reliable readings beyond 10 minutes for each sample.

Temperatures above 90 degrees C could not be used in the tests because they affected the polyethylene sheathing that surrounded the sample, and weakened the bonding material. This was discovered in the preliminary testing.

Figure 9 - The diamond drill press that was used to drill cores.

Figure 10 - One of the core samples obtained from the drilling.

Figure 11 - One of the cores, inserted into polyethylene sheathing.

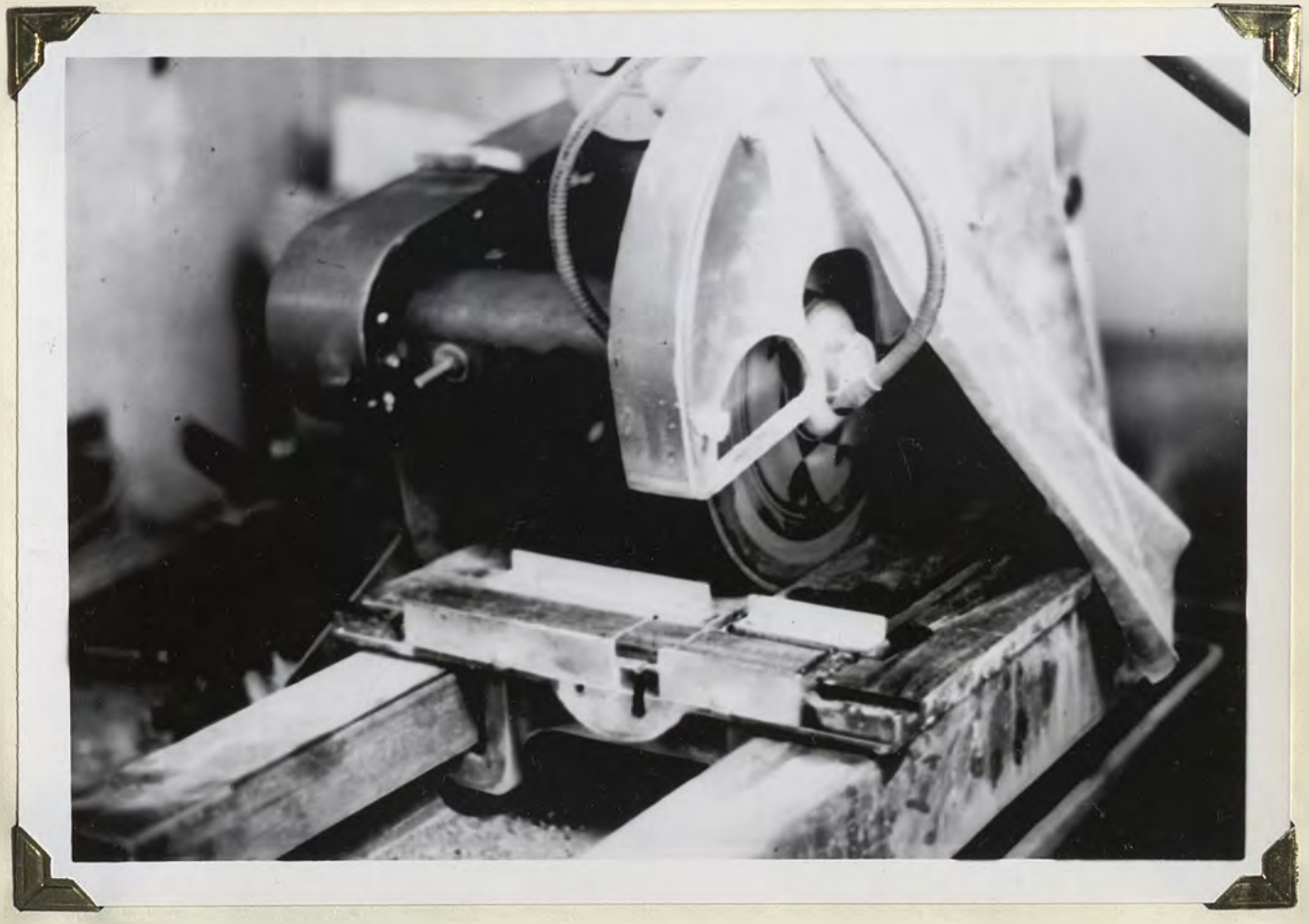

Figure 12 - The saw that was used to cut disks from the sheathed cores.

Figure 13 - Disks of sandstone, sheathed with polyethylene.

Figure 14 - The sample holder, containing the disk, shown within the oven.

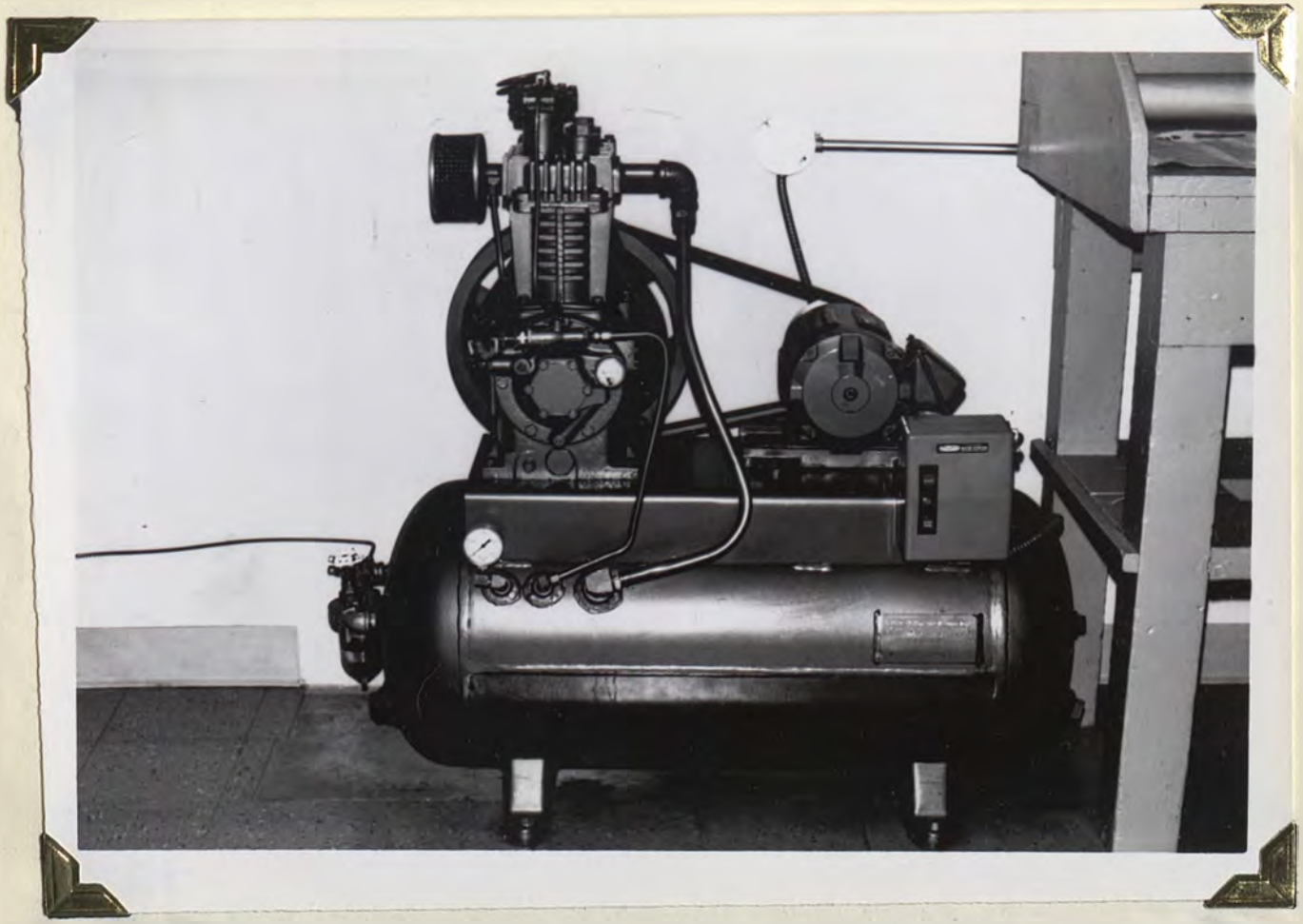

Figure 15 - The compressor that was used to generate the inlet pressure.

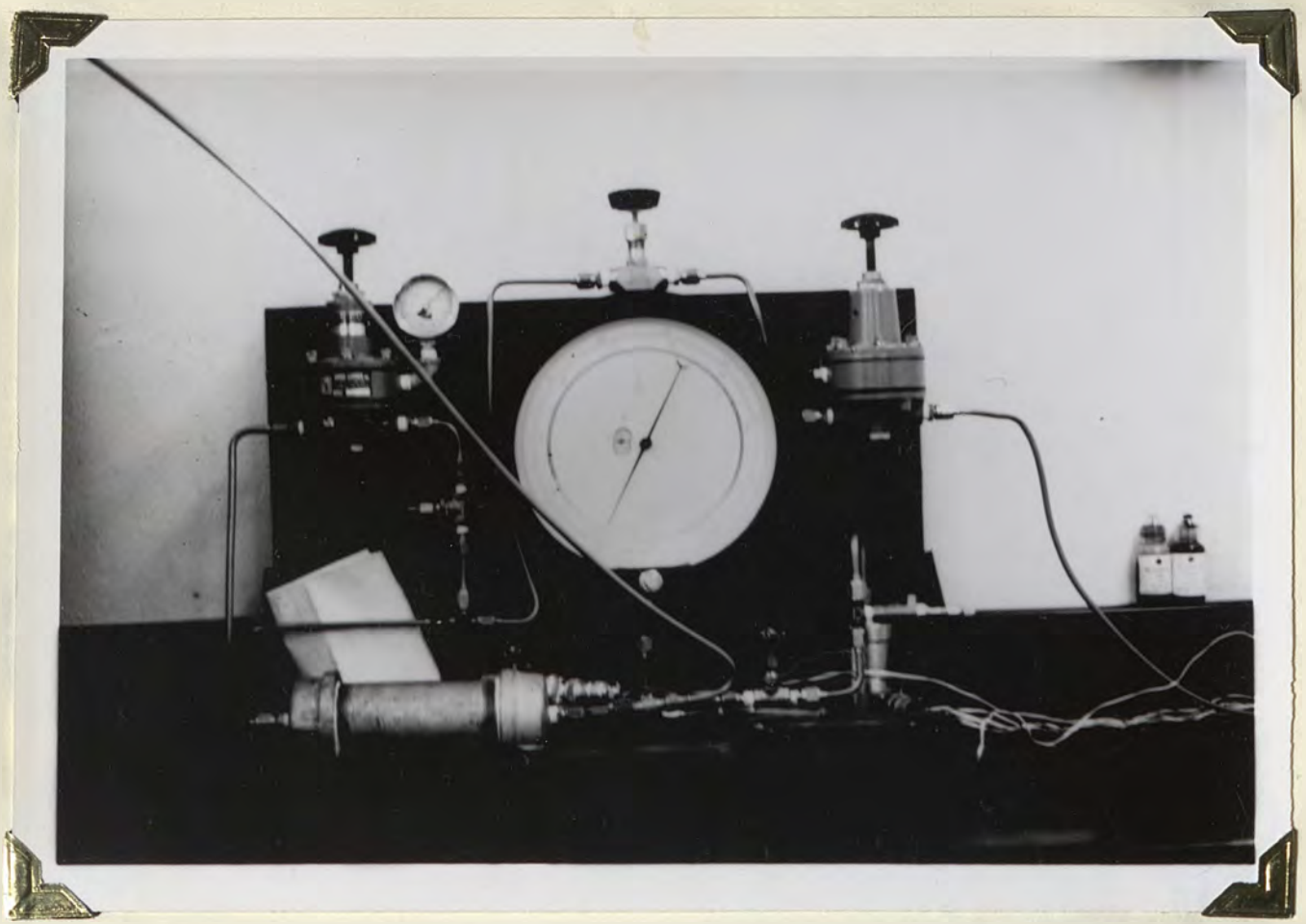

Figure 16 - The pressure regulator, the pressure guage, and the air drier, shown at the top, the middle, and at the bottom of the picture respectively.

Figure 17 - The wet test meter, used to measure the volume of the air passing through the sample in time t.

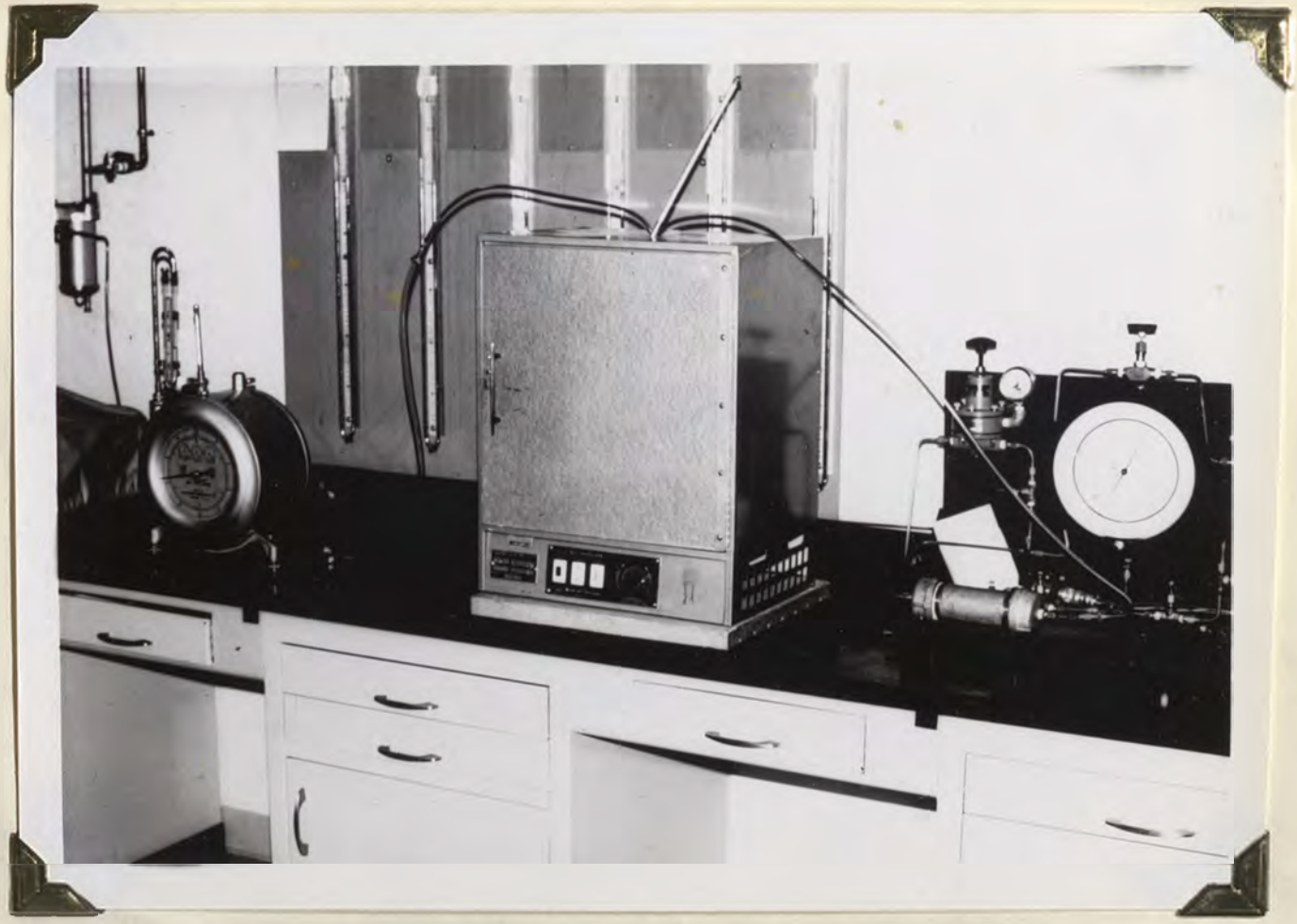

Figure 18 - A setup of the testing apparatus, from right to left, the pressure guage, the oven containing the sample, and the wet test meter. Also visible, are the connecting copper tubes, and the thermometer at the top of the oven.

RESULTS AND DISCUSSION

EXPERIMENTAL RESULTS

Data Tabulation

TABLE I

T=24 C,

P2=0.9987 atg,

u=0.1826 cP.

Obs #	Pl atg	Pm atg	Qm ml/sec	(1/Pm) l/atg	Ka mD
1	1.7007	1.3497	0.3737	0.7400	23.9795
2	2.3809	1.6898	0.4742	0.5918	15.4541
3	3.0612	2.0300	0.5805	0.4926	12.6783
4	3.7415	2.3701	0.6920	0.4219	11.3649
5	4.4218	2.7103	0.7443	0.3690	09.7945
6	5.1020	3.0504	0.8375	0.3278	09.1940
7	5.7823	3.3905	0.9208	0.2949	08.6709
8	6.4626	3.7307	0.9981	0.2680	08.2286

TABLE II

T=41 C,

P2=0.9987 atg

u=0.1912 cP.

Obs #	Pl atg	Pm atg	Qm ml/sec	(1/Pm) 1/atg	Ka mD
1	1.7007	1.3497	0.3178	0.7400	21.3529
2	2.3809	1.6898	0.4184	0.5918	14.2778
3	3.0612	2.0300	0.5224	0.4926	11.9468
4	3.7415	2.3701	0.5867	0.4219	10.0893
5	4.4218	2.7103	0.6608	0.3690	09.1052
6	5.1020	3.0504	0.7435	0.3278	08.5470
7	5.7823	3.3905	0.8175	0.2949	08.0607
8	6.4626	3.7307	0.8861	0.2680	07.6495

TABLE III

T=57 C,

P2=0.9987 atg

n= 0.1986 cP.

Obs #	Pl atg	Pm atg	Qm ml/sec	(1/Pm) 1/atg	Ka mD
1	1.7007	1.3497	0.3492	0.7400	24.3719
2	2.3809	1.6898	0.4602	0.5918	16.3132
3	3.0612	2.0300	0.5224	0.4926	12.4091
4	3.7415	2.3701	0.5886	0.4219	10.5137
5	4.4218	2.7103	0.6869	0.3690	09.8316
6	5.1020	3.0504	0.6922	0.3278	08.2651
7	5.7823	3.3905	0.7743	0.2949	07.9319
8	6.4626	3.7307	0.8402	0.2680	07.5333

TABLE IV

T=69 C,

P2=0.9987 atg

n=0.2035 cP.

Obs #	Pl atg	Pm atg	Qm ml/sec	(1/Pm) 1/atg	Ka mD
1	1.7007	1.3497	0.3143	0.7400	22.4763
2	2.3809	1.6898	0.4268	0.5918	15.5014
3	3.0612	2.0300	0.5108	0.4926	12.4330
4	3.7415	2.3701	0.5727	0.4219	10.4822
5	4.4218	2.7103	0.6261	0.3690	09.1821
6	5.1020	3.0504	0.6783	0.3278	08.2986
7	5.7823	3.3905	0.7588	0.2949	07.9633
8	6.4626	3.7307	0.8514	0.2680	07.8228

TABLE V

T=86 C,

P2=0.9987 atg

n=0.2115 cP.

Obs #	Pl atg	Pm atg	Qm ml/sec	(1/Pm) l/atg	Ka mD
1	1.7007	1.3497	0.2317	0.7400	20.6649
2	2.3809	1.6898	0.3829	0.5918	17.3444
3	3.0612	2.0300	0.4876	0.4926	14.8018
4	3.7415	2.3701	0.5668	0.4219	12.9384
5	4.4218	2.7103	0.6330	0.3690	11.5779
6	5.1020	3.0504	0.6721	0.3278	10.2552
7	5.7823	3.3905	0.7535	0.2949	09.8622
8	6.4626	3.7307	0.8289	0.2680	09.4983

Graphical Results

Permeability was plotted against temperature, inlet pressure, and the reciprocal of the mean pressure. The temperature and inlet pressure were found to have a nonlinear relationship with permeability, and the reciprocal of the mean pressure across the sample, was found to have a straight line relationship with permeability.

Regression analysis was used to plot the relationships. A Wang 602 plotter was used to draw the curves, after determining the type of general curve that had the best fit. Linear regression analysis was used to plot 1/Pm (reciprocal of mean pressure) versus permeability .

Permeability versus 1/Pm (mean pressure)

These results exhibited a high correlation coefficient, which indicated a fair degree of accuracy in the experimental results. These parameters were plotted as in figure 19, in order to determine the equivalent liquid permeability of the rock {2}.

@ T=24 degrees C (room temp.)

The following relationship was indicated from the results:

$K = 1.9720 + 22.2635(1/Pm)$

1.9720 is the equivalent liquid permeability value of the rock used in this test, the value of Ko (K at 1/Pm = 0) at infinite mean pressure across the sample.

@ T=41 degrees C

$K= 1.8469 + 20.5162(1/Pm)$

In this case the value of Ko was 1.8469

@ T=57 degrees C, The value of Ko was found to be below zero and is not presented. A negative value of Ko is physically impossible but nevertheless present due to insufficient sensitivity of the volume measuring device. Negative values of Ko were also found by other researchers, {2}, {8}.

@ T=69 degrees C

$K = 0.6529 + 24.2636(1/Pm)$

The equivalent liquid permeability value of the sample being, Ko = 0.6529.

@T=86 degrees C

The relationship was $K = 2.4367 + 25.0259(1/Pm)$

in this case the value of Ko was 2.4367.

As the graph in figure 19 indicates, there exists a straight line relationship between permeability and the

reciprocal of mean pressure across the sample.

When the temperature is increased from 24 degrees C to 41 degrees C, the overall permeability value drops. With a further temperature increase, the permeability increases, and the highest overall permeability values are indicated at the higher temperatures. This seems to be in line with reasoning and interestingly, if the plot at room temperature is withdrawn from the graph, the lines in figure 19 will exhibit a generally uniform increasing trend.

The Inlet Pressure Effect On Permeability

The relationship between permeability and inlet pressure was found to be a least square fit power curve (lny=ln(a)+bln(x)). This curve had a higher correlation coefficient than exponential and hyperbolic fits. The results indicated a decrease in the permeability value with an increase in the inlet pressure. The relationship between these parameters were not significantly affected by a change in temperature.

According to Darcy's law, $K \propto (Q/\Delta P)$. When the pressure increases the rate of flow registers an increase, but the increase in flow is less than the corresponding increase in pressure, hence the seemingly anomalous result.

The following equations were realized from the permeability, inlet pressure plot:

@ Room Temperature (24 degrees C) ln K = -0.7676ln(32.1767 Pl) for a correlation coefficient of -0.9822.

@41 degrees C

lnK = -0.7445 ln (28.7166Pl), the correlation coefficient being -0.9845

@ 57 degrees C

lnK = -0.8702 ln(35.4529 Pl)

at a correlation coefficient of -0.9875,

@ 69 degrees C

ln K = -0. 8032 ln(31.8235 Pl).

for a correlation coefficient of - 0.9875

and,

@ 86 degrees C

lnK = -0.6130 ln(28.9888 Pl).

for a correlation coefficient of -0.9972.

Figure 20 denotes the relationship between permeability and injection pressure. Permeability decreases with an increase in the injection pressure at every constant temperature level. This might be explained because permeability varies inversely as the pressure drop across

samples, and the lower the permeability value. At higher pressures, the volume rate of flow across the media increases, but apparently this increase is offset by the greater drop in pressure.

It is interesting to note that the permeability, injection pressure relationship; at constant temperatures, is similar to the relationships between permeability and the reciprocal of mean pressure drop across the media. As described earlier, the permeability decreases initially when the temperature rises from room temperature to 41 degrees C, but with a subsequent increase in temperature, there is a corresponding increase in the permeability value.

The Temperature Effect On Permeability

The temperature effect on permeability seemed to be rather erratic at first, but further investigation proved otherwise. Least curve plots did not yield any reasonable results, hence temperature was plotted against permeability using nth order regression analysis of the form

$$y = b(0) + b(1)x + \ldots\ldots + b(n)x^{n}$$

The following results were obtained, maintaining a constant inlet pressure in each case.

@ Pl = 1.7007 atg

$K = 77.9699 - 3.8873T + .0665T + 0.0005T - .0000197T + 0.0000001T$

@ Pl = 2.3809

$K = 49.72841984 - 2.553122T + 0.0481940T + .000184T - 0.000012T + 0.00000008T$

@ Pl = 3.0612 atg

$K = 22.11596217 - 0.6268114T + 0.0073334T + 0.0002047T - 0.00000508T + 0.00000003T$

@ Pl = 3.7415 atg

$K = 20.7393239 - 0.7684171T + 0.0213010T - 0.0002675T + 0.0000013T$

@ Pl = 4.4218

$K = 28.24177450 - 1.38025888T + 0.02604669T + 0.00011918T - 0.00000707T + 0.00000005T$

@ Pl = 5.1020 atg

$K = 11.729556 - 0.144159T + 0.000725T + 0.000066T - 0.000001T$

@ Pl = 5.7823 atg

$K = 12.341120 - 0.230764T + 0.002363T + 0.000075T - 0.000002T$

@ Pl = 6.4626 atg

$$K = 9.4304994 - 0.0330277T - 0.0019621T + 0.0000717T - 0.0000009T + \ldots.$$

The relationships between permeability and temperature follow a uniform trend as indicated by figure 21.

At the higher pressures, the increase in temperature beyond 41 degrees C causes a corresponding increase in permeability. At 1.7007 atg injection pressure, however, there exists a sinusoidal type of relationship between permeability and temperature, i.e. at 24, 57 and 90 degrees C are found maxima points, and at 32, and 83 degrees C, minima points, for the permeability values.
A similar type of relationship is evident at 2.3809 and 4.4218 atg injection pressures.

The curves at injection pressures of 3.0612, 3.7415, 5.1020, 5.7823 and 6.4626 atg depict a uniformly increasing trend for temperatures greater than 41 degrees C of the lixiviant. The permeability decreases, however, when the temperature rises from room to 41 degrees C.

The overall nature of the curves signify that a reduction in the permeability values are effected by an increase in the injection pressures. The decrease in the

permeability values are less significant at the higher pressures.

When the injection pressure increases from 1.7007 to 3.7415 atg , the permeability decreases by over 50% in value. Correspondingly when the injection pressure increases from 4.4218 to 6.4626 atg, the drop in permeability is less than 20%.

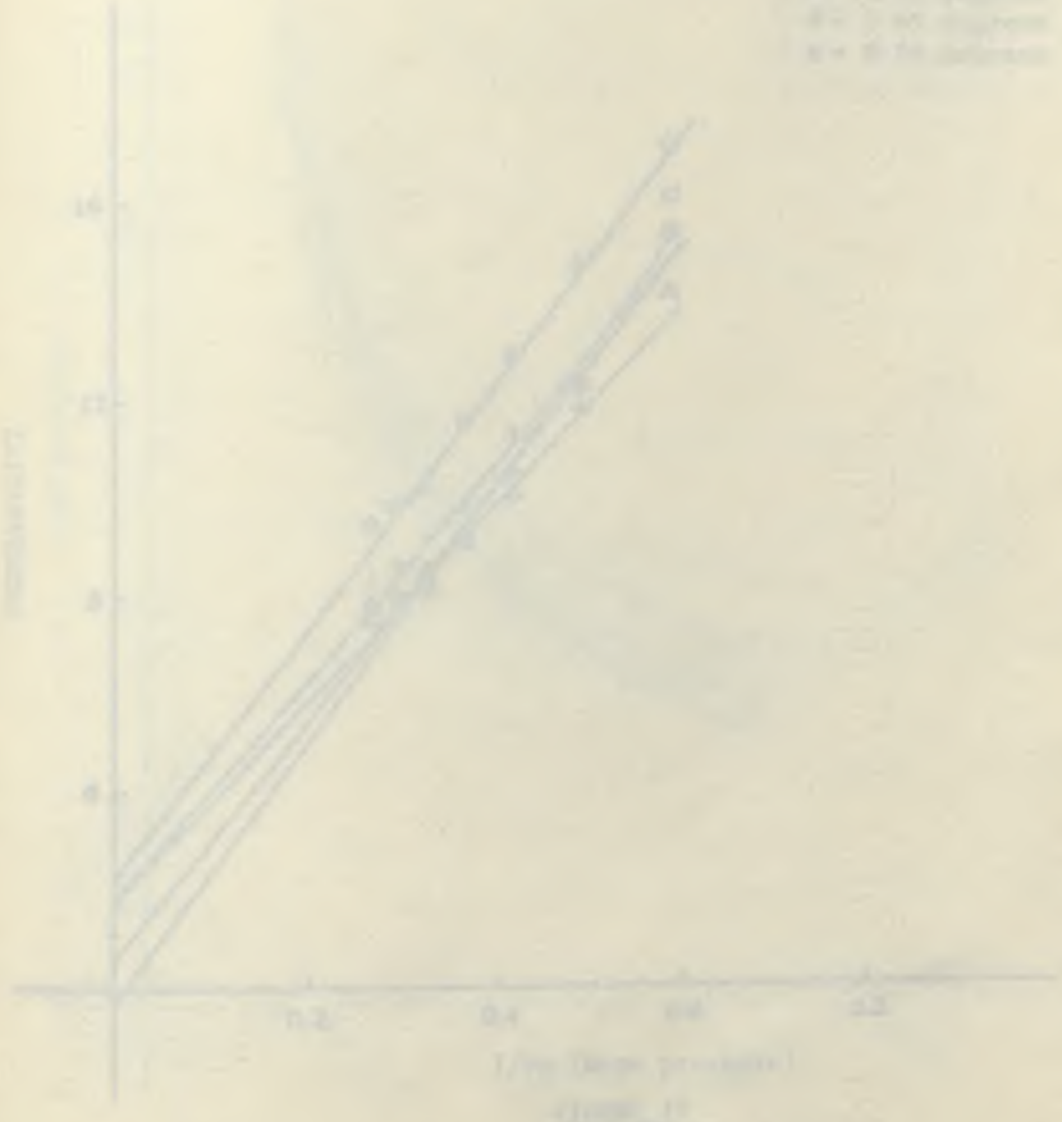

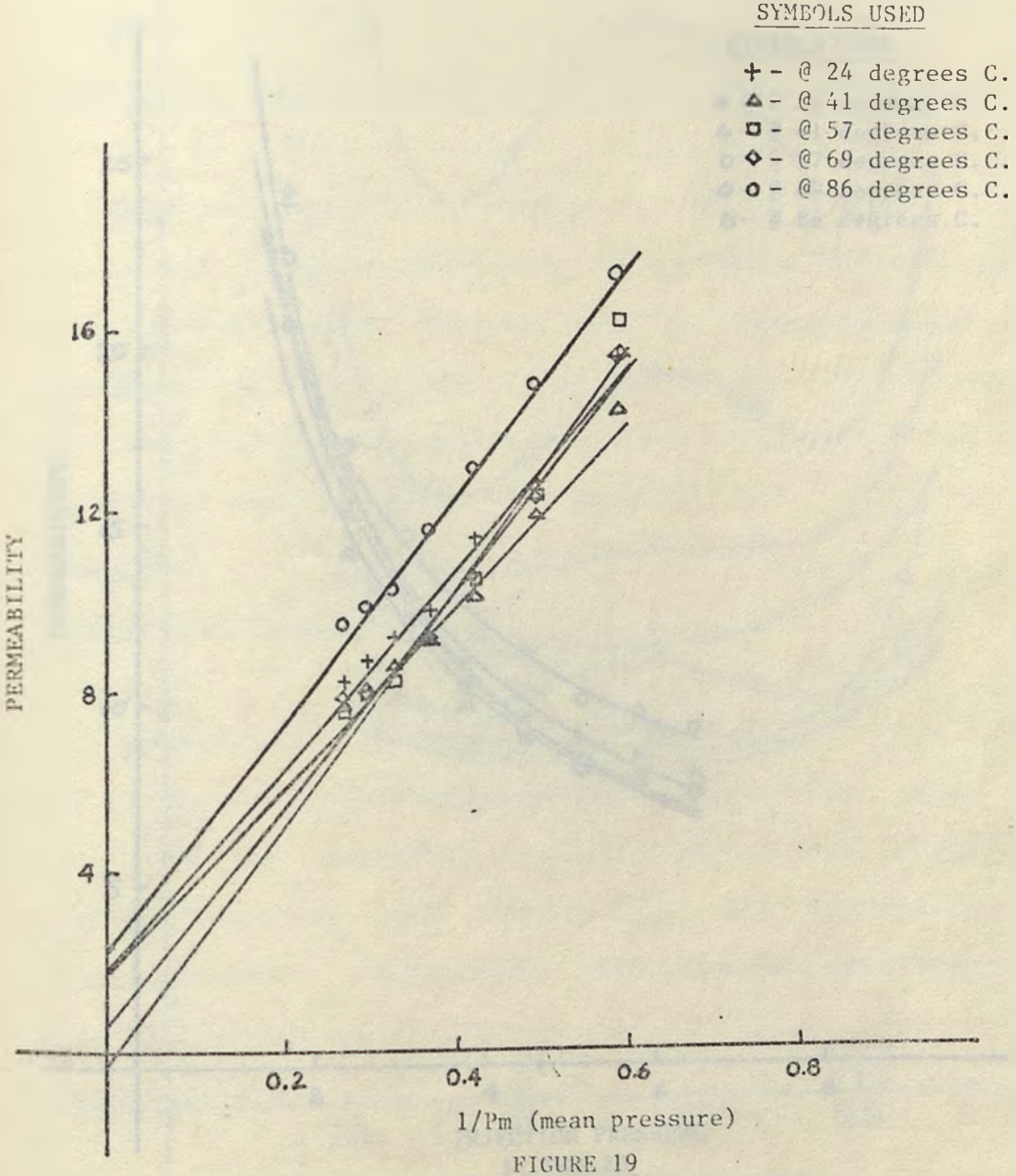
SYMBOLS USED
+ - @ 24 degrees C.
△ - @ 41 degrees C.
□ - @ 57 degrees C.
◇ - @ 69 degrees C.
○ - @ 86 degrees C.
PERMEABILITY
16
12
8
4
0.2
0.4
0.6
0.8
1/Pm (mean pressure)

FIGURE 19

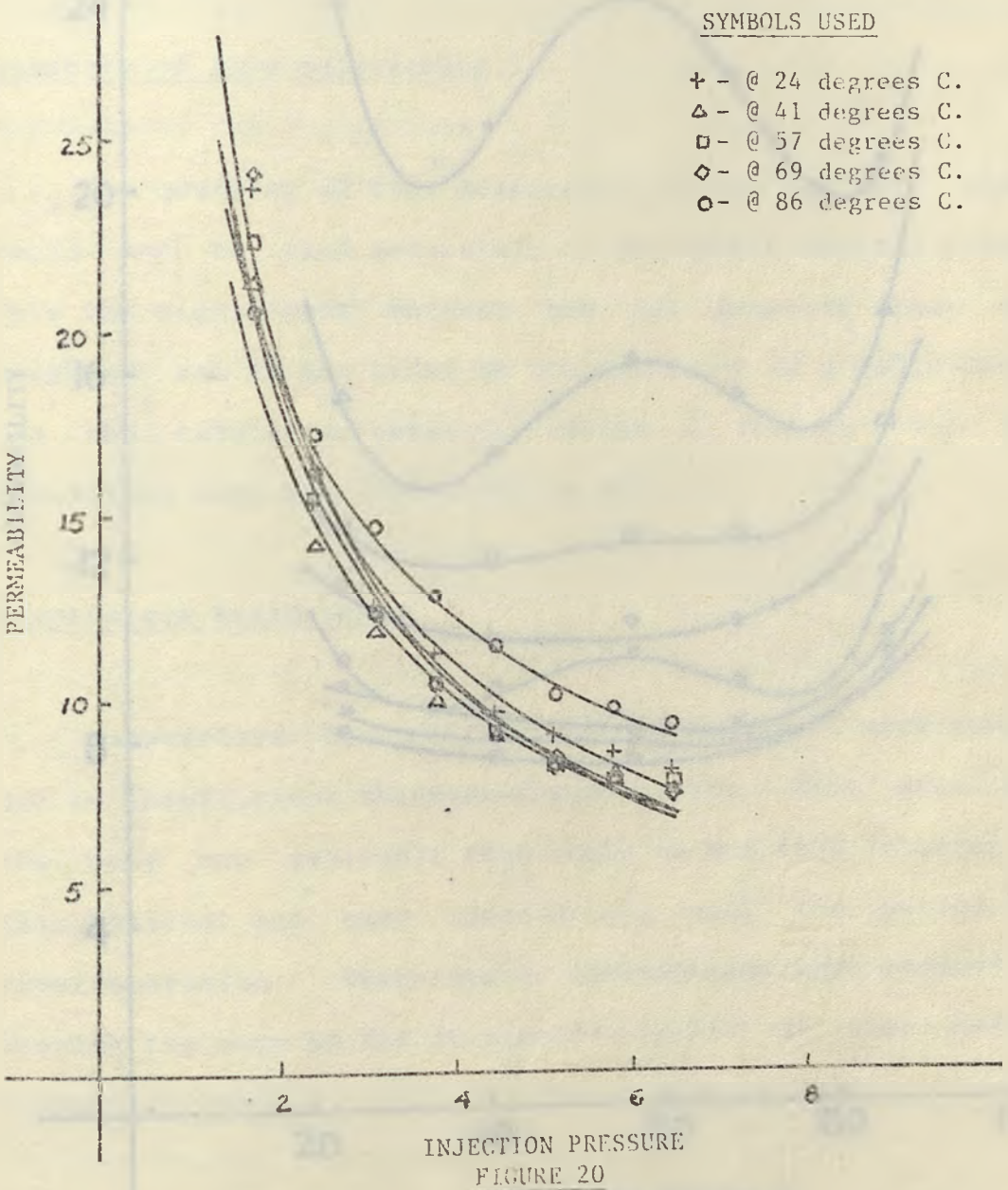
SYMBOLS USED
+ - @ 24 degrees C.
△ - @ 41 degrees C.
□ - @ 57 degrees C.
◇ - @ 69 degrees C.
○ - @ 86 degrees C.
PERMEABILITY
25
20
15
10
5
2
4
6
8
INJECTION PRESSURE

FIGURE 20

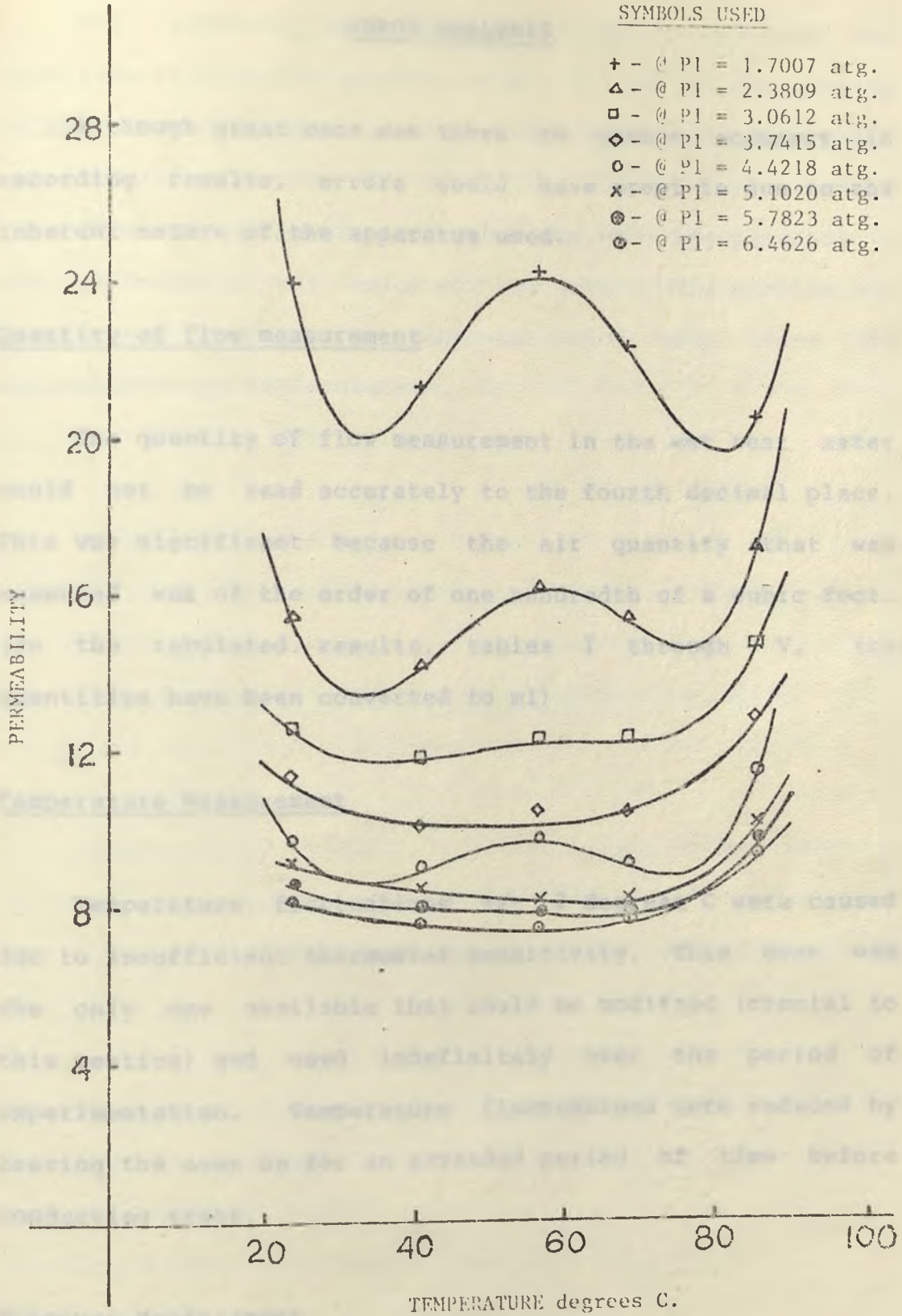
SYMBOLS USED
+ - @ P1 = 1.7007 atg.
△ - @ P1 = 2.3809 atg.
□ - @ P1 = 3.0612 atg.
◇ - @ P1 = 3.7415 atg.
○ - @ P1 = 4.4218 atg.
× - @ P1 = 5.1020 atg.
⊗ - @ P1 = 5.7823 atg.
⊙ - @ P1 = 6.4626 atg.
PERMEABILITY
28
24
20
16
12
8
4
20
40
60
80
100
TEMPERATURE degrees C.

FIGURE 21

ERROR ANALYSIS

Although great care was taken to ensure accuracy in recording results, errors could have crept in due to the inherent nature of the apparatus used.

Quantity of flow measurement

The quantity of flow measurement in the wet test meter could not be read accurately to the fourth decimal place. This was significant because the air quantity that was measured was of the order of one hundredth of a cubic foot. (In the tabulated results, tables I through V, the quantities have been converted to ml)

Temperature Measurement

Temperature fluctuations +/- 2 degrees C were caused due to insufficient thermostat sensitivity. This oven was the only one available that could be modified (crucial to this testing) and used indefinitely over the period of experimentation. Temperature fluctuations were reduced by leaving the oven on for an extended period of time before conducting tests.

Pressure Measurement

The pressure guage was sufficiently accurate and sensitive to keep the pressure within 0.1 psi of the testing value. These fluctuations were caused by the air compressor automatically shutting off when the accumulator pressure reached a certain level, and recharging when the pressure in the accumulator was below the low point. The problem was ameliorated by conducting experimentation only after the accumulator was fully charged.

SUMMARY AND CONCLUSIONS

Experimental Analysis

The laboratory model was designed indigenously in part, and after {2}, for the air permeability measuring device.

Sandstone was obtained from the vicinity of Las Vegas in Clark County, Nevada.

Cores were drilled by a diamond drill press, cut by a rotary blade saw, and sheathed with polyethylene for a snug fit in the sample holder. The diamond saw was again used to saw disks of about 1.5 cm in size, from the sheathed core. The disks were lightly polished, washed and oven dried.

Samples were tested in an air permeability measuring device. Injection pressure was generated by a compressor, and lixiviant temperature by an oven that enclosed the sample.

The coefficient of permeability was calculated from the relationship (equation (3)):

$Ka = Qm\ n\ L/\{A(P1 - P2)\}$

Qm was calculated using the expression (2) or,

$Q2\ P2 = Qm\ Pm$

Pm was the mean pressure drop across the sample, or

Pm = (P1 + P2)/2

Tables of permeability values were generated at different injection pressures for constant temperature conditions (see list of tables). From these tables the coefficient of permeability was plotted against temperature and injection pressure (figures 19, 20 and 21) .

Conclusions

Coefficient of Permeability and 1/Pm

These results were compared favorably with previous investigations {2}, {5}, {7} and {8}. The straight line relationship proves that permeability is inversely proportional to the mean pressure across the media.

The main purpose of plotting these relationships was to obtain the liquid permeability values of the rock samples, these were found to be

1.970 mD @ 24 degrees C.

1.8469 mD @ 41 degrees C.

negative @ 57 degrees C.

0.6529 mD @ 69 degrees C. and,

2.4367 mD @ 86 degrees C.

These results do not agree completely with those obtained by Weinbrandt {6}, primarily because different samples were used to conduct the experiments by the author; whereas, Weinbrandt, used a single sample for all his tests.
The reason for using different samples for each test is to obtain statistically, a confidence interval of one order of magnitude of mean value at 95% significance level, Larson {17}, specified that it was necessary to test at least 14 specimens, as an average.

Weinbrandt's results indicated a decrease in permeability, with an increase in temperature.
In the present investigation, the permeability values decreased initially upto 69 degrees C.
The higher value of permeability at 86 degrees C, could be interpreted either as continuous micropassages passing through the thickness of the sample, thus allowing more fluid to pass through than would otherwise be the case; another plausible explanation for the higher permeability value could be the insufficient sensitivity of the volume measuring device, the latter reason is stated, because @ 57 degrees C, a negative value of permeability was obtained, such a value was also indicated by Breese {2} and Larson

{8}.

Permeability Coefficient and Injection Pressure

An increase in the injection pressure caused a corresponding increase in the flow quantity through the media (see tables I through V), but caused a decrease in the permeability value of the samples (see figure 20), this decrease in the permeability value is because permeability varies inversely as the pressure drop across the media, thus the increase in the flow quantities effected by higher injection pressures is offset by a correspondingly larger increase in the pressure drop across the sample. This study would seem to suggest that higher injection pressures are favorable to the quantities of lixiviant flowing across the media, and hence should be adapted to increase production quantities, this is true excepting for the fact that the permeability values decrease, causing a lowering in the efficiency of the system. Thus, it is imperative that field tests be conducted in order to determine the most efficient injection pressure that is applicable to a particular situation, and adopt that injection pressure if it lies within the range necessary for the production value desired.

More experimentation is recommended in this field and

especially onsite testing, to obtain better and clear cut results.

Lixiviant Temperature and Permeability

These results were plotted without taking into account the expression of Klinkenberg, or Ka = Ko(1+b/Pm) (as was done in figure 19) and may explain the erratic nature of the plots (figure 21).

Sinusoidal types of relationships were obtained at the lower injection pressures of 1.7007 and 2.3809 atg, but as the pressure was increased, the curves stabilized and did not fluctuate as much. In fact, the increase in temperature (at higher injection pressures) cause an initial decrease (upto 41 degrees C) and then an increase in the coefficient of permeability across the sample.
Furthermore, at pressures beyond 5.1020 atg, the decrease in the permeability values were less significant than at the lower pressures.

It may be inferred from the above results that the lixiviant temperature causes erratic changes in the permeability values of the rock samples, at lower pressures, and stabilize at the higher pressure values, to cause almost no effect on the permeability values of the rock.

The author recommends that site testing be done because the viscosity values of liquid lixiviants could change appreciably with rises in temperature, as compared to that of air. Thus no reasonable directives can be issued in the face of the results obtained, the laboratory tests have however, proved invaluable in indicating that field tests on injection pressures and temperatures of the lixiviant could provide definite indications concerning the leachability of the ore deposit.

REFERENCES

{1} Larson, William C., "Uranium Insitu Leach Mining in the U.S.", IC 8777, Bureau of Mines IC/1978.

{2} Breese, Charles R., "A Study of Freeze-Thaw Characteristics of selected Nevada Mineral Aggregates," Engineering Report No. 38, Department of Civil Engineering, University of Nevada, Reno. August 1970.

{3} Scheidegger, Adrian E. "The Physics of Flow through Porous Media." New York: The Macmillan Company, 1960.

{4} Lubinski, A., "The Theory of Elasticity for Porous Bodies displaying a strong Pore Structure," Proc., Second U.S.National Congress of Applied Mechanics (1954) 247-256.

{5} Dolch, W. L., "Studies of Limestone Aggregates by Fluid Flow Methods," A.S.T.M. Proceedings, 59 (1959).

{6} Weinbrandt, R. M., Ramey, H. J. Jr., and Casse, F. J., " The Effect of Temperature on the Relative and Absolute Permeability of Sandstones," Society of Petroleum Engineers Journal, October 1975.

{7} Muscat, Morris, "Physical Principles of Oil Production." New York: McGraw Hill Book Company, 1960.

{8} Larson, T. D., Boettcher, A., Cady, P., Franzen, M., and Reed, J., "Identification of Concrete Aggregates Exhibiting Frost Susceptivility," Highway Research Board Program Report 15 (1965), 4-10.

{9} Zoback, M. B., and Byerlee, J. D., "Permeability and Effective Stress," American Association of Petroleum Geologists, Bulletin, January 1975.

{10} Knutson, C. F., and Bohor, B. F., 1963, "Reservoir Rock Behaviour under Moderate Confining Pressure," 5th symposium in Rock Mechanics, University of Minnesota: New York, Macmillan, p. 627-659.

{11} Brace, W. F., Walsh, J. B., and Francos, W. T., 1968 , "Permeability of Granite under High Pressure," Journal of Geophysics Research, vol. 73, no 6, p. 2225-2236.

{12} Vairogs, J., Hearn, C. L.,Dareing,, D. W., and Rhoades, V. W., 1971, "Effect of Rock Stress on Gas Production from Low Permeability Reservoirs," Journal of

Petroleum Technology, p. 1161-1167.

{13} Maclatchie, L. S., Hemstock, R. A., and Young, J. W., "The Effect of Compressibility of Reservoir Rocks and its Effect on Permeability," Trans. AIME (1958) 213, 386-388.

{14} Perkins, T. C., and Johnston, O. C., "A Review of Diffusion and Dispersion in Porous Media," Society of Petroleum Engineers Journal, March, 1963, p. 70-84.

{15} Bommer, P. M., and Schechter, R. S., "Mathematical Modeling of Insitu Uranium Leaching" paper presented at the AIME Annual Meeting, New Orleans, Louisiana, February 18-22, 1979.

{16} Longwell, C. R., Pampeyan, E. H., Bowyer, B., and Roberts, B., R. J., "Geology and Mineral Deposits of Clark County, Nevada," Bureau of Mines Bull. No. 62, 1965.

APPENDIX

STRESS STATE AROUND A WELL BORE IN POROUS MEDIA

Studies of the state of stress around the well bore in porous media have been done by Lubinski {4}, and more recently others. Lubinski's stress equations will be presented here.

He defined macrostress, S , as the average intensity of force per unit area of area, and microstress, S', as the average intensity of force per unit area of the interpore material. The third type of stress was called the effective macro stress, S''.

Consider macrostresses first. According to Lubinski, the strain in a porous medium subject to formation stresses (macrostresses) is given by,

$$Sr = (1/E)\{ Sr - (S\theta + Sz)\} + \{(1-2\nu)/E\}(1-\beta-\phi)\, p \quad \text{--- (A1)}$$

$$S\theta = (1/E)\{ S\theta - (Sr+Sz)\} + \{(1-2\nu)/E\}(1-\beta-\phi)\, p \quad \text{--- (A2)}$$

$$Sz = (1/E)\{S\, z - (Sr+S\theta)\} + \{(1-2\nu)/E\}(1-\beta-\phi)\, p \quad \text{--- (A3)}$$

where:

$$\beta = \{(1-2\nu i)/Ei\} \,/\, \{(1-2\nu)/E\}$$

The shear strain is given by

$$\gamma r\theta = (1/G)\tau\, r\theta \quad \text{--- (A4)}$$

$$\gamma \theta z = (1/G)\tau\, \theta z \quad \text{--- (A5)}$$

$\gamma_{rz} = (1/G)\tau_{rz}$ --- (A6).

These relationships are similar to those used in thermal stress studies for which impermeable bodies are subjected to surface forces and temperature. Because of this similarity, equations from thermal stress studies can be modified and used to determine stresses in porous rock.

Using the thermal stress equations, we find that the triaxial microstresses near a well bore are described by:

$$Sr = (1-\beta)\{1-2\nu)/(1-\nu)\}(1/r^2)\{(r^2-rw^2)/(rd^2-rw^2)\}\int_{rw}^{rd} prdr - \int_{rw}^{r} prdr\} - rw^2 rd^2 (pw-pd)/(rd^2-rw^2)(1/r^2) + (rw^2 pw - rd^2 pd)/(rd^2-rw^2) + \phi p + \{(rd^2)/(rd^2-rw^2)\}\{(rw^2/r^2) - 1\}(Sf-pd)$$ --- (A7)

$$S\theta = (1-\beta)\{(1-2\nu)/(1-\nu)\}(1/r^2)\{\{(r^2+rw^2)/(rd^2-rw^2)\}\int_{rw}^{rd} prdr + \int_{rw}^{r} prdr - pr^2\} + \{rw^2 rd^2 (pw-pd)/(rd^2-rw^2)\}(1/r^2) + (rw^2 pw - rd^2 pd)/(rd^2-rw^2) + \phi p - \{(rd)/(rd-rw)\}\{(rw/rd)+1\}(Sf - pd)$$ --- (A8)

$$Sz = (1-\beta)\{(1-2\nu)/(1-\nu)\}\{\{(2/(rd^2-rw^2)\}\int_{rw}^{rd} prdr - p\} + \phi p - So$$ --- (A9)

The last terms in equations (A7) and (A8) account for horizontal formation loading through impermeable boundaries, whereas the last term in equation (A9) accounts for

overburden loading through impermeable boundaries. These terms were superimposed on Lubinski's equations. When Lubinski derived his equations, he considered stress and flow through an open cyclindrical rock capped with impermeable horizontal boundaries. For example, without the last term in equation (A7), r at r = rd is $-(1-\phi)$ pd. With the last term included, in equation (A7), at r=rd is $(-Sf + \phi pd)$. The symmetry causes the shear stresses to be zero, not that the three stress components depend on the pressure distribution, which is to be determined. Let us now assume that the macrostresses can be determined, and consider how microstresses and effective stresses are determined from them.

Microstresses are related to macrostresses by the following simple relationships:

$$Sr' = Sr/(1-\phi) \text{ --- (A10)}$$

$$S\theta' = S\theta/(1-\phi) \text{ --- (A11)}$$

$$Sz' = Sz/(1-\phi) \text{ --- A(12)}$$

The effective stresses are determined as follows, consider Sr' to have two components such that $Sr' = p + S''r$ where p is the pore pressure and S''r is the effective radial stress --- (A13),

then substituting for the microstress r' gives

$$Sr'' = Sr/(1-\phi) - p \quad \text{--- (A14).}$$

Thus in the r direction (as in the z and θ) we can view the original microstress Sr' as the sum of two microstresses having components of Sr'' and p. thus also

$S\theta'' = S\theta/(1-\phi) - p$ --- (A15) and

$Sz'' = Sz/(1-\phi) - p$ --- (A16).

The microstress state on a cubical element in a reservoir can be divided into two microstress states; one in which the matrix in the cube is completely surrounded inside and out, by pressure equal to the local pore pressure, and another in which the microstresses are Sr'', $S\theta''$ and Sz'', with no pore pressure.

It is reasonable to assume that confining pressure does not affect the permeability and porosity of the rock appreciably. Hence porosity and permeability vary mainly due to Sr'', $S\theta''$ and Sz''.

The corresponding macrostresses, called effective stresses are:

$$S_r''' = (1-\phi)\, S_r'' = S_r - (1-\phi)\, p \quad \text{---} \quad (A17)$$

$$S_\theta''' = (1-\phi)\, S_\theta'' = S_\theta - (1-\phi)\, p \quad \text{---} \quad (A18)$$

$$S_z''' = (1-\phi)\, S_z'' = S_z - (1-\phi)\, p \quad \text{---} \quad (A19)$$

Since the laboratory tests were performed on dry samples, the pore pressure was zero, hence the effective stresses were the same as the stresses produced on the sample due to the pressure drop across the sample.